An Environmental case study of the Inner Drammensfjord: Environmental conditions and microplastic accumulation - Drammensfjorden, Eastern Norway

Åshild Grammeltvedt Hamre

Thesis submitted for the degree of
Master of Science in Environmental Geoscience
60 credits

Department of Geoscience
Faculty of Mathematics and Natural Sciences

University of Oslo

September, 2021

An Environmental case study of the Inner Drammensfjord: Environmental conditions and microplastic accumulation - Drammensfjorden, Eastern Norway

Åshild Grammeltvedt Hamre

September, 2021

Photo by Martine Thorstensen, August 2020.

An Environmental case study of the Inner Drammensfjord:

Environmental conditions and microplastic accumulation -

Drammensfjorden, Eastern Norway

https://www.duo.uio.no/

Printed: Reprosentralen, University of Oslo

Abstract

Microplastic has become a well known term the last decade, but how well known is the issue of microplastic pollution into the marine environment? An attempt on determining the microplastic accumulation in Drammensfjorden and its evolution through industrialisation, were done by collecting sediment cores in Drammensfjorden, August 25th, 2020. The impact of the industrialisation can be mirrored by the sediment accumulated in the same period of time. Polymers stay hidden in the sediment to tell the story of over-polluted rivers and poorly handled waste. The accumulated plastic polymers can give an overall picture of pollution into the fjord throughout history. How the environmental condition of Drammensfjorden change in times of industrialisation, and if it has changed since introducing framework regarding contamination of the fjord.

Sediment cores were collected at 80 meters water depth with a Gemini-twin-corer, field parameters of the water column were taken with a CTD-device. The core DRA2A was sub-sampled in intervals of 1 or 2 cm slices. Samples were frozen before freeze dried, for less disturbance of the sediment.

The samples were treated with hydrogen peroxide for organic material removal. A density separation process was done with the help of NaI solution, to separate possible microplastic form the sediment. The lab process produced four separate glassfiber filter papers per sample, which were manually picked and described for observed microplastic through microscope. A portion of the picked microplastic was tested with Raman and FTIR spectroscopy, to determine the type of plastic.

The results of the identification of microplastic were inconclusive, due to oxidation of iodide contaminating the material, both Raman and FTIR spectra struggled to identifying the polymers.

The sediment core was dated according to research done by Norconsult in 2018/19. The visual data indicated higher accumulation of smaller particles down core. The characteristics in shape of the observed microplastics had a shift when the industrialisation of Drammen happened, and the introduction of synthetic polymers in the industry. The establishment of treatment plants appears to have a direct correlation with the accumulated microplastic in the sediment, as a decrease in microplastic in the core can be seen shortly after the establishments.

Comparing microplastic observed in DRA2A with microplastic in samples taken closer to the harbour in Drammen at 60 meters water depth, show accumulation of larger quantities, and higher density microplastic. Larger particles and fragments dominate the samples taken closer to shore, compared to smaller fibers further out in the fjord.

The CTD-data measured very low concentrations of oxygen in deep water, and close to the seafloor. Drammensfjorden is closed off from the larger Oslofjord by glacial moraines at Svelvik, which causes very low circulation in deeper waters. The low concentrations of oxygen classifies the environmental condition of the fjord as "Very Bad", which does not give the true condition of the fjord, due to the lack of circulation in deeper water.

Acknowledgement

I would like to thank my supervisors;
Helge Hellevang, Professor at the Department of Geosciences, UiO.
Elisabeth Alve, Professor at the Department of Geoscienses, UiO.
Niels Højmark Andersen, Senior Engineer, Department of Chemistry, UiO.
Amy Lusher, Researcher at NIVA.
Rachel Hurley, Researcher at NIVA.
For help with sample collection, lab-methods, analysis and questions throughout the process of making this thesis.

I would also like to thank the crew at F/F Trygve Braarud for a pleasant day out on Drammensfjorden, and making the sampling possible during COVID-19 restrictions.

Thank you to Mufak Said Naoroz at the Sediment-lab at the Department of Geoscienses for help during lab work.

Thank you to Post Doctoral Researcher, Sebastian Primpke at the Alfred Wagner Institute, for helping with the identification of Raman and FTIR spectra.

I also have to thank Martine Throsensen for long hours in the lab, and sharing frustrations through the work with our theses.

I would like to thank my parents for teaching me the importance of curiosity regarding nature and nature mechanisms. For supporting me during my studies. And for guiding me through difficult days, when motivation was low.

Thank you to my grandparents for always reading my reports, for interesting discussions and hard questions. And a special thank you to my grandpa for understanding geological terms, and showing genuine interest in my work.

Last but not least, thank you to my boyfriend for putting up with me throughout the process of writing my thesis.

Åshild Grammeltvedt Hamre
Department of Geoscienses, UiO, September 1st 2021.

Contents

List of Figures

List of Tables

1 Introduction

The word "plastic" was first used for easily shaped and pliable compounds, before the first synthetic polymer was created in 1907. The first synthetic polymer made was called Bakelite and patented in 1909, to accommodate the demand for ivory and silk (H. Davis, 2015). Bakelite was first used as an substitute for on-demand material, but later on incorporated with other compounds to change the physical and chemical properties of the product. Plastic have grown to be the worlds most used material (Crespy et al., 2008).

1.1 Plastic and microplastic

Plastic as a resource compared to other materials is cheaper, lightweight, durable and strong. During the last century the demand for plastic have grown exponentially, so have the questions regarding the environmental impact of the product (H. Davis, 2015). Plastic polymers comes in a wide range of types, most of them mixed to fit the demanding properties of the product. Six polymers makes up almost 80% of today's plastic production (Kershaw et al., 2019):

1. Polyethylene (HDPE and LDPE)
2. Polypropylene (PP)
3. Polyvinyl chloride (CVC)
4. Polyurethane (PUR)
5. Polystyrene (PS)
6. Polyethylene terepthalate (PET)

The worlds plastic demand can be divided into eight categories:

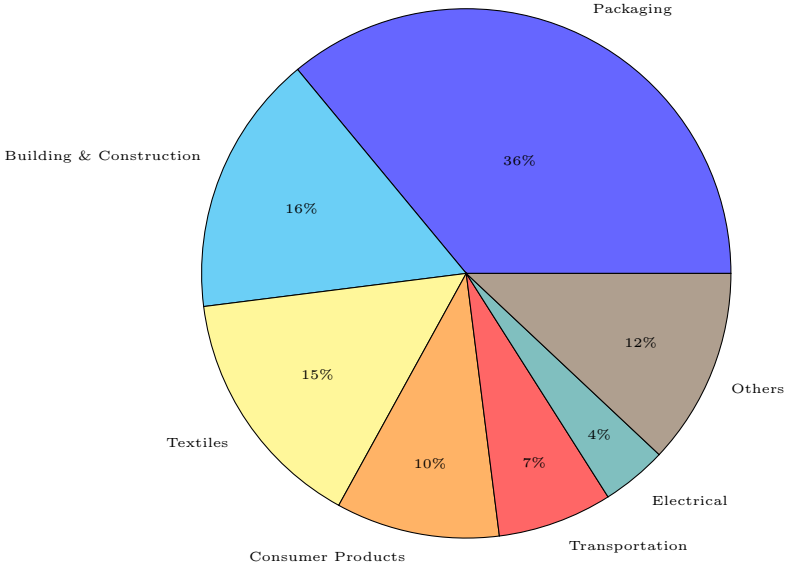

Global demand on plastic products, and market sectors. "Others" include appliances, medical, mechanical engineering etc. Modified after Geyer et al., 2017; Kershaw et al., 2019.

Plastic as marine litter can be categorized in several sizes.

Table 1.1: Size categories of plastic marine litter, from (Gregory and Andrady, 2003; Kershaw et al., 2019).

Field descriptor	**Relative size**	**Common size division**	**Measurement units**
Mega	Very large	$>$ 1 m	Meters
Macro	Large	25-1000 mm	Meters Centimeters Millimeters
Meso	Medium	5-25 mm	Centimeters Millimeters
Micro	Small	$<$ 5 mm	Millimeters Microns
Nano	Extremly small	$<$ 1 µm	Nanometers

In this report, plastic in the size range of microlitter and smaller will be the main focus. The name "microplastic" was first used by Thompson et al., 2004 in 2004, and referred to microscopic plastic particles. Years later, in 2009 Arthur et al., 2009 determined a size limitation for "microplastic", which referred to plastic particles in the size range of microlitter and smaller (Table 1.1). First in 2011 Cole et al., 2011 introduced a refined definition based on origin. Microplastics were divided into two subgroups; primary and secondary microplastics. Primary microplastics refers to plastics that are originally produced to be of microscopic dimentions. Secondary microplastics on the other hand refers to fragmented or degraded plastics.

1.1.1 Marine microplastic pollution

Microplastic as a pollutant in ocean sediments might originate from different industrial waste, or waste in general. According to Ziccardi et al., 2016, there are two specific origins of microplastic; manufactured or fabricated plastic pellets and fragmentation (primary microplastics) or/and degradation of plastic waste (secondary microplastics). Consumer plastics are very often "single-use plastics", and end up in the oceans, either as direct loss into the ocean, from for example the fishing industry, or transported from land deposits by rivers and streams (Ribic et al., 2010; Watson et al., 2006). According to J. R. Jambeck et al., 2015, an estimate of 4.8 to 12.7 million MT plastic waste entered the ocean in 2010 only. A new estimate was made by Borrelle et al., 2020, where 19 to 23 million MT entered the oceans in 2016. The first consequence concerning plastics in the marine environment were sea animals and birds ingestion of plastics.

1.1.2 Types of plastic

Plastic can be divided into several categories, synthetic polymers, biodegradable polymers, semi-synthetic polymers and bio-based polymers. The difference between them are the degradation or degradation rate, where the synthetic polymers are barely degradable or not degradable at all, and the biodegradable polymers degrade quite easily in comparison.

Table 1.2: Synthetic polymers (non-biodegradable plastic), and area of use, from (Shah et al., 2008).

Plastic polymers	**Uses**
Polyethylene (PE)	Plastic bags, water bottles, plastic wrap, toys, drainage pipes, and plastic containers for oil.
Polystyrene	Disposable cups, packaging materials, laboratory ware, some electronic use.
Polyurethane	Tires, bumpers, used in refrigerator insulation, sponges, cushions for furniture, life jackets.
Polyvinyl chloride	Seat covers in cars, shower curtains, raincoats, bottles, shoe soles, garden hoses.
Polypropylene	Bottle caps, drinking straws, medicine bottles, car seats, car batteries, bumpers, disposable syringes, carpet backings.
Polyethylene terephthalate	Soda bottles (for carbonated drinks), pillow and sleeping bag filling, some types of jars, textile fibers.
Nylon	Speedometer gears, windshield wipers, helmets, inks, rainwear, cellophane, clothing.
Polycarbonate	Street lighting, safety visors, rear lights for cars, houseware, greenhouse roof, can be used in lenses in glasses.
Polytetrafluoroethylene	Different industrial applications, coating on nonstick kitchen utensils.

Table 1.3: Biodegradable polymers (plastic), and area of use, from (Disha et al., 2012).

Plastic polymers	**Uses**
Polyglycolic acid (PGA)	Controlled drug release, implantable composites, bone fixation parts.
Polylactic acid (PLA)	Packaging and paper coatings, sustained release systems for pesticides and fertilizers.
Polycaprolactone (PCL)	Agricultural films, slow-release systems for drugs.
Polyhydroxybutyrate (PHB)	Products like bottles, bags, wrapping film and disposable nappies, controlled drug release carriers.
Polyhydroxyvalerate (PHBV)	Films and paper coating, biomedical applications, therapeutic delivery of worm medicine for cattle, release system for pharmaceutical drugs, and insecticides.

1.1.3 Degradation

Degradation of plastics is a process of removing, dissolving, and breaking down particles. According to Andrady, 2011, there are several types of degradation:

1. Biodegradation – action of living organisms (e.g. microbes)
2. Photodegradation – action of light (e.g. sunlight in outdoor exposure)
3. Thermooxidative degradation – slow oxidative breakdown at moderate temperatures
4. Thermal degradation – action of high temperatures
5. Hydrolysis – Reaction with water

These mechanisms are happening naturally in different environments. The most common mechanism in fjord sediments is biodegradation. Biodegradation can occur in sediments through microbial activity under specific conditions. The biodegradable plastics mentioned in table 1.3 can be broken down in the sediment under both oxygenated and non-oxygenated conditions, the product in the two scenarios are different. For well-oxygenated conditions the polymers can result in humus, CO_2 , and H_2O. Biodegradation in anoxic or non-oxygenated conditions often results in methane gas (CH_4), CO_2 , H_2S, NH_3, and H_2 as well as water. The process of biodegradation in anoxic conditions is more complex than for well-oxygenated conditions (Disha et al., 2012; Shah et al., 2008).

1.2 Drammensfjorden

In this thesis the accumulation of microplastic in Drammensfjorden will be the main focus. Drammensfjorden is located in the eastern part of southern-Norway. The area of Drammen was, due to its location close to the fjord, one of the earlier industrialized cities in Norway. The inner part of Drammensfjorden is almost closed off from the larger Oslofjord, by glacial moraines close to Svelvik, south in Drammensfjorden. The moraine limits the circulation in the deeper parts of the fjord, and therefore makes the sediments close to anoxic (Hvoslef et al., 1987).

The inner Drammensfjord can be divided into two main river basin areas; Drammenvassdraget area and the Lierelva area. These two areas infiltrates the northern part of the fjord, where the Drammen basin area (Drammenvassdraget) is located in north-west, and the river of Lier (Lierelva) in the north-east. Both the water chemistry and the ecological and the chemical status in the inner Drammenfjord is classified as bad, as of 22.01.2021, and rechecked 27.08.2021 (The Norwegian Water Resources and Energy Directorate (NVE), 2021b).

1.2.1 Drammen watershed

The main rivers draining into Drammensfjorden are Lierelva and Drammenselva, both rivers contribute with possible environmental and microplastic contamination from the surrounding area. Both rivers have separate watersheds, where the smaller river Lierelva have a significantly smaller drainage area than Drammenselva. The watershed of Lierelva (no. 011) extends over Lier municipality, and covers an area of 306.91 km^2 (Fig. 1.1 **b.**). The main distributor of drainage water into the fjord comes from Drammenselva, a watershed with a size of 17 106.33 km^2. The watershed extends from Beitostølen in north to Holmestrand in south and Finse in west to Raufoss (Gjøvik) in east (Fig. 1.1 **a.)**. The watershed, called Drammensvassdraget (no.012) is the third largest watershed in Norway in areal and the second largest in amount of yearly precipitation (The Norwegian Water Resources and Energy Directorate (NVE), 2021a; Aagaard et al., 2001).

Due to the large surface area of the Drammensvassdraget watershed, the possible plastic contamination sources are many. The main source of plastic pollution to the fjord will still be the industrial activity surrounding the fjord.

1.2.2 Industrial activity

Potential sources of microplastic pollution in the Drammen area could be industrial manufacturing as well as poorly handled waste management. Back in the early industrialisation of Norway, Drammen was one of the biggest industrial cities. Before the 1980's one-third of the working residents in Drammen were industrial workers. Some of the earlier industrial pollution sources can therefore be; "Drammen Slip og Verksted", "Drammen paper mills", "Norsk kabelfabrikk", among others (Industrimuseum.no, N.D). Records show that lumber was shipped from Drammen as early as the 1300s, and the first factories were established in the mid to late 1800's (Wøhni, 2007). The early industrialisation of Drammen makes the foundation of the city, and also the pollution of the fjord. As the industry of the city grew, so did the contamination sources into the fjord. The financial top for the industry of Drammen was at the beginning

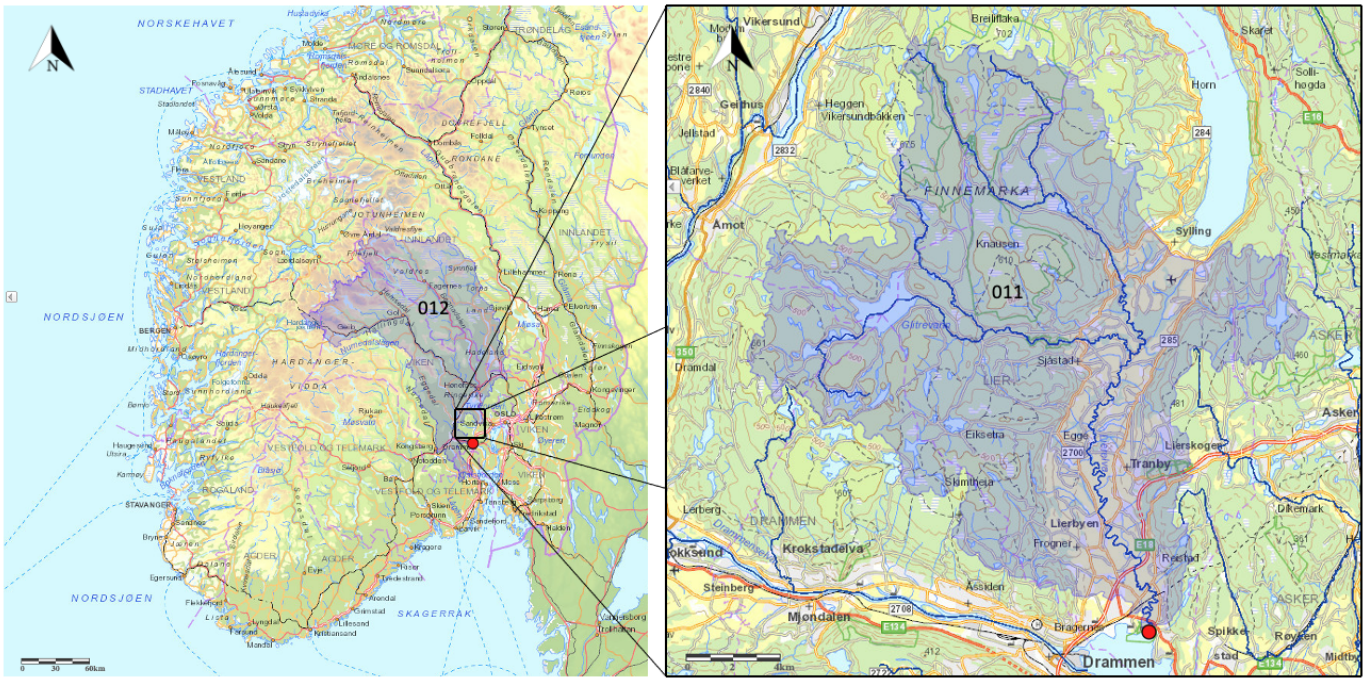

Figure 1.1: Areal surface of **a.** Drammensvassdraget no.012 compared to **b.** Lierelvvassdraget no.011 . Modified from (The Norwegian Water Resources and Energy Directorate (NVE), 2021a).

of the 1900's (Borgen, 2004b; Heieren, 2004a). According to Wøhni, 2007, there were at one point 15 paper factories with direct waste drainage into Drammenselva, which drains out in Drammensfjorden. This gives an indication of large volumes of waste draining into the fjord and therefore may indicate particles of manufacture waste in fjord deposits. There are also records showing that sewage from approximately 100 000 citizens drained directly into Drammenselva. In the late 1980's measures were made to reduce the contamination of the river, and to make the city environment better. After the measures taken to clean the city of Drammen, one can hope that the contamination of the fjord and the sediments will show a significant change in a short time span (Spigseth and Miljøverndepartementet, 2007; Wøhni, 2007).

1.2.3 Drammen as a plastic manufacturer

Throughout the industrial history of Drammen, several factories manufactured products containing synthetic polymers. Factories operating during the 1900's usually drained straight into the fjord, without any treatment or filtration. The same for the sewage. Some of the first synthetic polymers, such as rubber was introduced already in 1915, while polyester, nylon and polypropylene were introduced in the 1950's. Some specific sources of plastic contamination of Drammensfjorden, in the early "plastic-age" could be (Fig. 1.2):

Rubber manufacturer. "Brodahl's gummivarefabrikk" was first established in 1915, and quickly became a big competitor as a rubber manufacturer. Brodahl's gummivarefabrikk was the first producer of rubber balls in Norway, the company also produced rubber strips, and washing sponges made out of rubber. "Refsum's gummivarefabrikk" was established in 1925, the manufacturer mainly produced rubber balls, soles and rubber heels, as a direct competitor to Brodahl's. Refsum's gummivarefabrikk was well known for being the first company to extrude **neoprene** commercially (Fredriksen, 1966). Refsum's was the main distributor of rubber heels in Norway, before the war. Raw material restrictions following the war, made it difficult to maintain the large production of rubber products. The product range were therefore limited to rubber soles and heels as well as rubber parts for industrial machines. In the years following the war, the rubber factory focused their production on rubber strips for fridges and washing machines, as well as rubber gaskets. The manufacturer grew, and in the 1970's it became the largest rubber manufacturer after the Viking group. The company was sold to Mehren-rubber in 1986, before the factory was moved to Sande in 1988. Shortly after Refsum's factory was moved, Brodahl's factory was closed due to competition from the Asian market (Borgen, 2011; Heieren, 2004b).

Packaging manufacturer. The early production of packaging in Drammen, started already in the 1870's. Packaging such as wooden boxes and pharmacy glass, wrapping paper and paper bags were first produced, before introducing polymers. The first plastic packaging came into the market in 1947, produced by "Star Paper Mills". The new plastic packaging was a direct competitor for the already existing pergamyn paper, manufactured by the same company (Borgen, 2004c; Borgen, 2011).

Fiberglass reinforced plastic. In 1954 a company named "Birger Næss Plastvarefabrikk" started manufacturing motorcycle helmets made out of fiberglass reinforced plastic. The polymer used in reinforcement with fiberglass was **polyester**. The helmets were introduced to the market shortly after the manufacturing of fiberglass reinforced boats. The company later expanded their product range with safety and skiing helmets as well as smaller boats and custom orders. In 1966 BirgerNæss Plastvarefabrikk was sold and merged with "Teknisk Isolering" (Ticon). In the early 1970's polyester was replaced with **polycarbonate** due to cost efficiency. The production was in 1979 moved to Italy, and the production in Drammen ended. Even though the production of motorcycle helmets came to an end, Teknisk Isolering started producing helmets for firefighters, and invested in larger constructions for the aluminum industry, made out of fiberglass reinforced with polyester and **vinylester** (Borgen, 2004d; Borgen, 2011; Heieren, 2020a).

Transparent packaging. Transparent plastic packaging and bags were first produced in 1955 by the newly established company "A/S Transparent Emballasje". During the 1950's raw materials such as plastic polymers was hard to get in Europa, the newly established company therefore had to import **polyethylene** from the US. They produced plastic packaging by extruding the polymers and shaping it into transparent plastic film or plastic bags. The raw material

shipped from the US came as dry granulate, and of higher quality than the European material. The company started producing snack packaging for "Maarud" in 1961, as of 2011, the company, now under a new name, still produces packaging for Maarud (Borgen, 2011; Heieren, 2020c).

Early plastic bags. Vopa, "Vokspapir fabrikken", also called Foilpack Vopa, was one of the first in Drammen, and Norway, to manufacture plastic bags. Vopa was also the first manufacturer to produce plastic wrap. The production of plastic bags fully started in 1963, by "Vopa", "S.Hammer" and "Star Paper Mill". Star Paper Mill, as the first manufacturer of plastic packaging in Drammen later on, bought both companies S. Hammer and Vopa in 1967 (Borgen, 2004c; Borgen, 2011; Heieren, 2004c).

Christmas decorations. In the years following the war, an import bans led to new product demands in Norway. "Jul-i-Nor" was established in 1945, due to import ban of decoration ornaments. The company produced holiday decorations, packaging tape and Christmas glitter. From the 1950's the packaging tape was made with **polypropylene** (Borgen, 2011; Heieren, 2020b).

Machine felt with synthetic fibers. A company named "Den Norske Papirfiltfabrik" was established in 1916, due to the increasing demand of felt in the paper industry. The company first produced technical felt made out of wool, and later, in 1965, introduced synthetic polymers. Polyamide fiber, **nylon** was first introduced to strengthen the felt, to make the felt more heat resistant, polyesters such as **terylene** was incorporated. The factory was closed in 1979, due to decreasing demands of industrial felt (Borgen, 2011; Kristoffersen, 1966).

Textile, clothing and shoe industry. The textile industry exploded in Drammen in the early 1930's, over 20 newly established factories, amongst them; Wool, cotton, leather, clothing, shoes, galoshes and rubber, fur, felt and coloring factories. "P. Christensen tricotagefabrik" was established in 1892 in Kristiania (Oslo), but later moved to Drammen in 1907. The main production for P. Cristensen tricotagefabrik was knitwear and stockings, the factory also had its own departments for coloring, spinning, weaving, washing and repairs. The company used several types of materials for their different products, such as cotton, wool, leather and rubber. Later on the company introduced **nylon** when making stockings. In 1965 P. Christensen tricotagefabrik merged with "A/S Pedersen og Dekke" which was located in Bergen. The factory in Drammen mainly used cotton as a fabric material, while Bergen used wool. P. Christensen and its production was moved permanently to Bergen in 1967, and the factory was transformed into a shopping mall. The Textile, clothing and shoe industry in Drammen decreased rapidly from 1970 to 1990, due to competition from lower income countries, with lower production costs (Borgen, 2004a; Borgen, 2011).

1.2.4 Wastewater and sewage handling.

According to chief-engineer Helle Egeberg Várli in the water and sewage department in the municipality of Drammen, the city of Drammen had a modern

Figure 1.2: Industrial activity in the area of Drammenselva, during the mid 1900's, draining out in the fjord. Potential sources of plastic pollution of the fjord. Modified from Google Earth.

water supply system, already in 1865. As the demand of regional water from the district, the need for individual septic tanks grew. This led to contamination of smaller streams and lakes in local areas. During the 1800's all sewage and wastewater was led directly into streams, rivers or into the fjord by pipes, some of them still intact today. When the smaller streams and rivers became too contaminated, the streams were put in pipes and led directly into Drammenselva.

The industrial activity in Drammen grew considerably in the 1900's. Wastewater and sewage from the factories were also led directly into Drammenselva. The sewage and wastewater included excess water from production, and cleaning water containing production residue. As a consequence of all the contamination from both privet households and the factories, Drammenselva was amongst the most polluted rivers in Norway in the 1950's and 60's.

The first larger treatment plant in Drammen, **Muusøya renseanlegg** (Fig. 1.3), was established in 1978, after the municipality came up with framework for sewage and wastewater in 1972. Muusøya treatment plant is a chemical treatment plant, located at Muusøya, upstream in Drammenselva. Muusøya is responsible for treating sewage and wastewater for the Åssiden district and part of Gulskogen.

With the framework for sewage and wastewater, the goal was to improve the quality of the river and the fjord. By 1986, only 23 % of sewage and wastewater were cleaned or treated by treatment plants. Therefore in 1987 a new revised

framework plan was implemented to ensure the future quality of the river and fjord (DrammenKommune, 2018). The revised framework suggested two main focuses:

1. Network of pipelines with pumping stations and weirs along the river and fjord, to capture wastewater from pipelines draining directly into the river or fjord.

2. Build a new treatment plant at Solumstrand, located by the west shore of Drammensfjoren.

(H.E. Varí, Personal communication, 05.08.2021)

The new treatment plant, **Solumstrand renseanlegg** (Fig. 1.3), was built in 1994, and by 1995 the framework from 1987 was terminated. At this point approximately 97% of the inhabitants in Drammen connected to one of the two chemical treatment plants.

Figure 1.3: Treatment plants in Drammen today. Muusøya established in 1978, and Solumstrand established in 1994 and renovated in 2008-2011. Modified from Google Earth.

In the late 1990's and early 2000's a new environmental focus started, whilst the investment in sewage and wastewater decreased. Parts of the pipeline network separated weirs from sewage, upstream this was not the case, therefore the treatment plants had to treat a lot more water than necessary, and the costs

became too high. With heavy rain showers the treatment plants were overflowing and drained excess wastewater into the river or fjord. This issue was first handled in 2003 when new framework came in to force.

Renovation of the Solumstrand treatment plant started in 2008, the renovation was extensive due to transition from chemical to biological treatment. It was also necessary to keep the treatment plant functional during the renovation, therefore the remodel of Solumstrand was complete in 2011.

In 2014 the municipality of Drammen developed a model of the drainage network, to calculate discharge from weirs (H.E. Varí, Personal communication, 05.08.2021).

1.3 Hypothesis - Study aims

The main focus of this thesis was to determine the accumulation of microplastic in sediments over time. As well as determining the environmental condition of the fjord based on oxygen content in the water column. The amount of microplastic in the sediment core gives an indication of the accumulation of plastic contamination in time, and therefore reflect the pollution of the fjord over the years.

The area of interest in this thesis was Drammen and the fjord of Drammen, which is known as one of the first cities to industrialize. It is therefore likely that the accumulation of plastic in the sediments of the fjord started soon after.

Several hypothesis´ were tested:

1. Microplastic count in the sediment increase downwards in the sediment core, and reflect higher pollution of plastic in the earlier days of industrial activity along the fjord of Drammen.

2. The sediment core collected date back to before industrial activity, and therefore lack microplastic down core.

3. Microplastic found in the sediment mirror the industrial production of the Drammen area.

4. The environmental condition of the fjord has improved during the last decades, following environmental measures introduced by the municipality of Drammen.

This thesis was partly done in collaboration with another student (Thorstensen, 2021). Mainly field and lab work were done in collaboration, to reduce costs.

2 Methods

The methodology of picking and classifying microplastic in this thesis will be divided into four parts.

1. Sample collection
2. Sample preparation
3. Plastic analysis
4. Classification of microplastic

2.1 Collection of samples

The samples described in this thesis were collected during a one-day cruise August 25th, 2020. Research vessel F/F Trygve Braarud, University of Oslo´s largest research vessel, was used in the collection of several sediment cores in the Inner Drammensfjord (Fig.2.1). The specific location of sample collection was based on previous reaserch done by NIRAS for Drammen and Lier kommune in 2019 (Ekeroth et al., 2020).

The two cores described in this thesis were first named after the location in the report by NIRAS, therefore the name 5Bx. Further on in this paper, the sediment cores will be refereed to as DRA2A and DRA2B.

Figure 2.1: Map over Drammensfjorden, and sampling site DRA2 (Modified from Kartverket.no).

2.1.1 Collection of sediment cores and field parameters

Sediment cores were collected with a Gemini-Twin Corer (Fig. 2.2a). The Gemini-twin corer could collect two cores at a time, with a maximum sediment

depth of 80 cm and a diameter of 8 cm. A CTD device (Fig. 2.2b) was deployed, in to collect additional data on conductivity, temperature and density within the water column at each location.

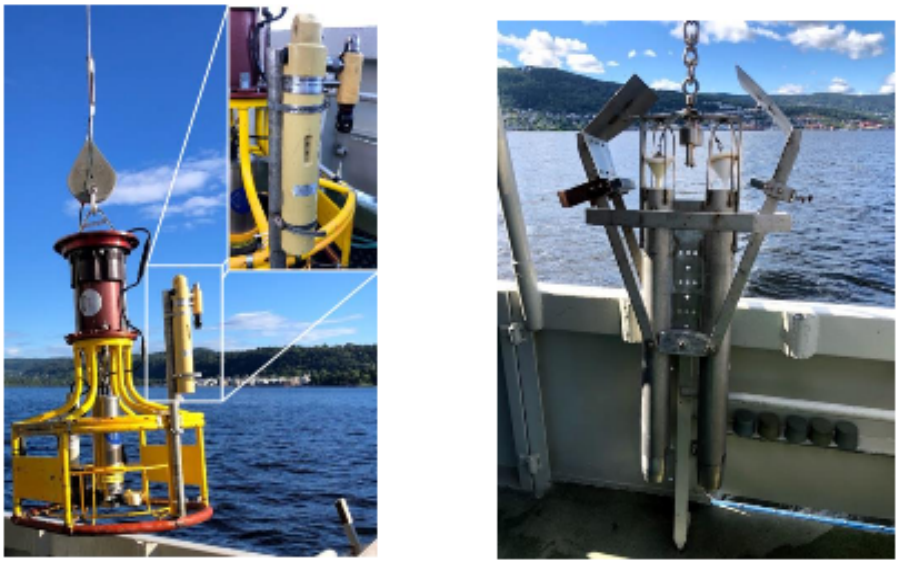

Figure 2.2: **a.** CTD-device deployed to collect CTD-data. **b.** Gemini-twin corer used to sample the sediment cores from the Inner Drammensfjord.

2.1.2 Sediment cores - 5Bx/DRA2

Location: *N 59°43.003' E 010°17.484'*
Depth: *80 meters*
Deployment speed: *0.7 m/s*
Time of collection: *09.40-10.10*

All sediment cores collected at this location were visualised inside plexiglass cylinders (Fig.2.3a), before deciding which cores would be sub-sampled and which cores to use for sediment logging (Fig.2.3b).

2.1.3 Preparation of sampling boxes

Before sample collection, boxes were weighed, and washed with 1 µm filtered water. The washing was done to prevent contamination from the surroundings to collect in the sampling boxes. The water was filtered to secure and ensure contamination free washing water, without particles.

The machine that filtrated the water used for washing, is called a millipore, which filtrates tap water to the desired "cleanliness" with the help of a Vent filter MPK01.

Weighing of the boxes were done to be able to calculate the water content for each sediment fraction of the collected core. Each box was labeled and weighed to the nearest 0.001g, before rinsed out with the filtrated water. The weight measurements were also used to correct for salinity.

Figure 2.3: **a.** Sediment cores collected at station 5Bx, three deployment, six cores- one inconclusive(5BxD). **b.** Sediment core 5BxA pushed out on deck for sediment logging.

2.1.4 Blank-tests

A Blank-test is a sample of a substance, or a sample who collects possible contaminants from the surrounding. There were taken a blank-sample of the water used for washing the sampling boxes. This blank-test was analyzed by NIVA (Norwegian Institute for Water Research) to determine if there was any contamination of the water.

Blank-samples were also taken during the sampling of the sediment cores. Cleaned sampling boxes were filled with filtered water, and kept nearby while sampling, these blanks were also analysed at NIVA. These tests were analysed to determine contamination factors and to prevent bias during sampling.

2.1.5 Sampling

Two cores at the desired location were chosen for further sub-sampling. Sediment core 5BxE and 5BxF,later renamed DRA2A and DRA2B, were chosen, due to less smearing of the top sediment inside the plastic casings. Each of the cores were sliced thin in centimeter thick sediment slices, for the fist 20 cm, and 2 cm slices for the remaining core length, and transferred to pre-washed boxes. Figure 2.4 shows an illustration of the sub sampling method, where the sediment is pushed upwards in the casing, before centimeter intervals of sediments were sliced. For each slice of sediment, the surface was described in respect to color, depth, shine and smell.

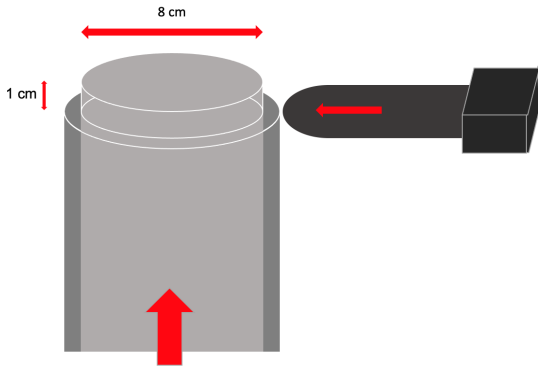

Figure 2.4: Illustration of the sampling method used for sub-sampling of the sediment cores.

2.2 Sample preparation

The laboratory methods used in this thesis were based on the procedure of the Norwegian Institute for Water Research (R. Hurley et al., 2018; NIVA, N.D).

2.2.1 Freeze drying

After sampling the sediment cores, the samples were put directly into the freezer. The frozen samples were freeze dried in two machines, *Christ Alpha 1-4LD pluss* and *Christ Alpha 1-4* (Fig. 2.5). Each sample was weighed frozen, before removing the water by freeze drying the samples.The freeze driers can be found in the sediment lab at the Department of Geosciences, UiO.

By freeze drying the samples, instead off drying them in an oven, the sediment in the samples was made sure to be undisturbed. In the freeze drying process the water particles moved directly from solid phase to gas phase, and therefore would not compromise the state of the sediment. After the water was removed from the sediment, each sample was weighed to determine the water content for the sediment fraction.

2.2.2 Water content calculation

The water content of the two sediment cores DRA2A and DRA2B were calculated by weighing the freezed samples before freeze drying, and the dry weight of the sediment after freeze drying. The percentage of water at each depth were therefore calculated according to equation 2.1.

$$\frac{Sediment_{wet} - Sediment_{dry}}{Sediment_{wet}} \times 100 = \text{Water content}(\%) \tag{2.1}$$

2.2.3 Blank-tests and background contamination

During lab sessions the colors of clothing were noted down to be aware of every possible contamination source of microplastics and fibers. Background contamination from the surroundings could result in unwanted particles in the samples. To monitor procedual contamination from the settling airborne plastic particles,

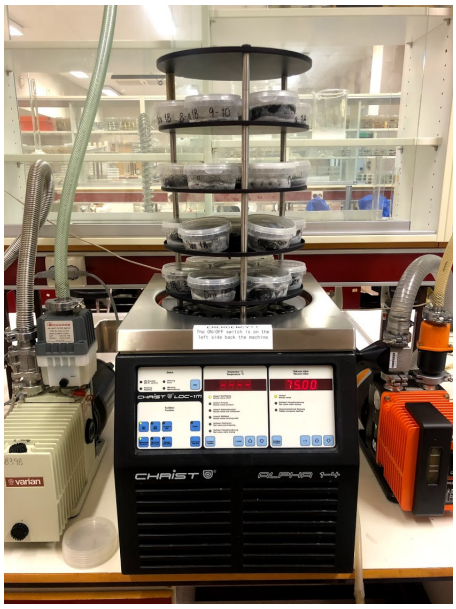

Figure 2.5: Freeze drying in the *Christ Alpha 1-4*, where 28 samples can be dried at a time.

petri-dishes with damp filter papers were placed in areas where the samples were exposed to potential contamination (e.i uncovered during the process of sampling, weighing, processing in the lab and during picking and characterization. The petri-dishes used for contamination control would with high probability contain the same particles as the contamination particles in the samples. By looking at the filter paper in a microscope, the particles were identified and could therefore be accounted for and disregarded in the sample.

2.2.4 Organic material removal - OMR

Removal of organic matter form the sediment samples was performed by using 30 % Hydrogen peroxide H_2O_2. The freeze dried sediments were carefully homogenised by stirring, before transferred to a Erlend Meyer flask. Hydrogen peroxide was then added to each sample in small increments, between 20-70 ml of H_2O_2 per sample (Fig. 2.6). The addition of hydrogen peroxide reacted with the organic material in the sediment and started fizzing and bubbling. After some time, often a couple of hours, when the fizzing calmed down, more hydrogen peroxide was added. For the reaction to happen faster, the Erlend Meyer flasks with sediments and hydrogen peroxide were put on a heating top. The optimal temperature for this reaction is between 10 and 40°C. The temperature of the heated Erlend Meyer flasks was monitored with thermometers, to make sure the temperature of the samples was within the optimal range for the reaction. After the fizzing and bubbling in the samples ended, the samples were taken off the heater. Filtered water was added, approximately 100-200 ml, depending on the flask and the fraction of liquid in the sample. The solution was then stirred or shaken, carefully not to spill any solution, before they were left over night for the sediment to separate from the liquid.

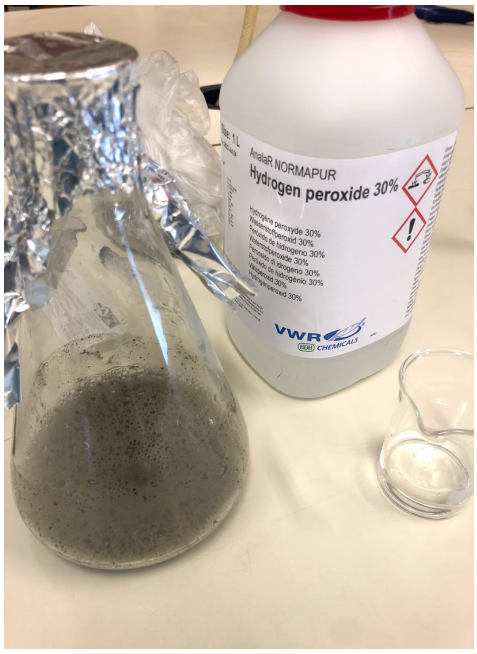

Figure 2.6: Organic material removal by using 30 % Hydrogen peroxide.

2.2.5 Freshwater filtration

Freshwater filtration was performed when the sediment in the sample had settled and the liquid were visually clear, typically within 24-72 hours, depending on the organic content remaining in the sample.

The samples were filtered with the help of a millipore and a pump (Fig.2.7). The filters used in the filtration process were *Whatman GT6* filters made out of glassfiber, with a 47 mm diameter and pore size of 47 µm. The filtrated sample was transferred to a 50 ml tube(s) and added more filtered water. The sediment captured in the filter was also transferred to the same tube. Every sample was aggregated by shaking the tube. The samples were left over night for a new separation to occur, before again, filtering the leftover liquid. The freshwater filtration was done to clean out the rest of the hydrogen peroxide in the sample. The importance of removing remaining hydrogen peroxide was done to ensure that the NaI would not react with the remaining hydrogen peroxide, which could ruin the sample. This process could be repeated several times, to ensure that the reagent was completely removed. Filters used in this procedure needed to be analysed in case of low-density plastic and particles floating in the freshwater. The low-density particles have a density lighter than water, with a proximate density of 1.0 g cm^{-3}, could then be found in these filters.

2.2.6 Making the NaI solution for Density separation

Sodium Iodide solution was made by adding 0.5 liter of filtered water to a beaker or a 1-2 litre Erlend Meyer flask. Before handling the crystallized NaI, it was important to wear protective gear, as it could cause irritation, allergic reactions or asthma symptoms if it came in contact with skin or was inhaled. Half of the

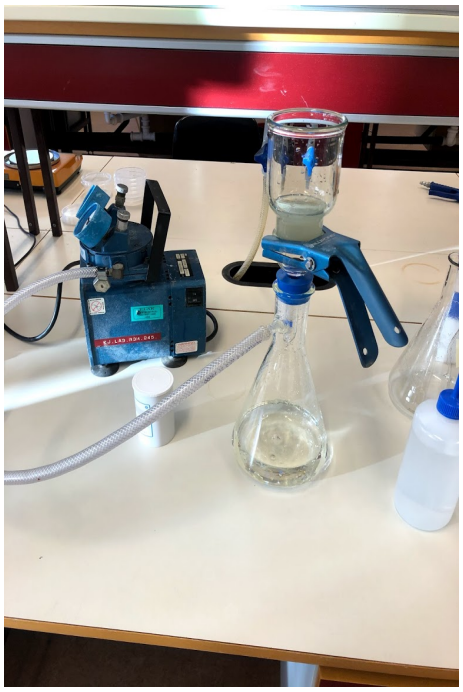

Figure 2.7: Fresh water filtration using millipore and *Watman GT6* filter with a 47µm pore size.

desired amount of the NaI, in powder form, were weighed before carefully added to the water. The solution was then shaken and stirred until the solution became clear and the salt was dissolved. The rest of the NaI, and the filtered water, were then added, in turns, until the the solution reached about 900ml. The density of the solution was checked two or three times, and adjusted by adding of water or more concentrated NaI until the density fell within acceptable limits. The desired density of the NaI solution in this case was 1.8 g cm^{-3}, where 10 ml of the solution weighed approximately 18 grams.

Before adding the Sodium Iodide solution to the samples, the solution was cooled, and filtered to remove possible contamination from the surroundings (Fig.2.8). The same filters were used for this filtration, 47µm pore size, as for the freshwater filtration of the samples.

2.2.7 Density separation

The density separation process was done with the help of a density separation solution consisting of Sodium Iodide and filtered water. The desired concentration was made with a ratio of approximately 80g NaI and 100 ml of filtered water. The density of the NaI solution was heavier than the plastic particles, the particles lighter than 1.8 g cm^{-3} floated to the top.

Each 50 ml tube containing the samples were added NaI solution. The tubes were filled up until it reached 0.5 cm from the top, to make sure all material were included in the liquid. After adding the solution, the samples were aggregated extensively to mix the sediment and the solution. The samples were then left

Figure 2.8: Filtration of Sodium Iodide solution by using millipore.

over night to separate. The process of density separation with NaI solution was repeated to make sure all the higher density particles were removed from the samples.

2.2.8 Filtration

After each round of density separation, the liquid fraction of the samples were filtered through a 47 µm filter paper, the particles with a lower dencity than the NaI solution would float to the top, and get trapped in the filter paper for further analysis. This procedure was repeated a second time to make sure all the high-density particles were separated from the soil in each sample.

2.2.9 Recycling of the NaI solution

The NaI solution used in the density separation process could be recycled by reducing the solution. The NaI solution filtered from the samples was transferred to a beaker or an Erlend Meyer flask, and put on the heater. The solution was then weighed to determine the density. When the desired density was reached, the solution was left to cool down, before filtered. The NaI solution was then ready to be reused.

2.2.10 Drying

The 47µm filter papers used in all stages of the method, were placed in petri-dishes and could be dried in several ways. One way of drying the filter papers was to put the petri-dishes, containing the filter paper, in an oven at 40°C for a couple of hours, with the lids slightly open for the liquid evaporating out of

the container, and prevent contamination of particles from the surroundings. An other option used to dry the filter papers was to let them air dry in room temperature for a few days, with the lids slightly open for the vapor to evaporate out of the container. The samples were covered with a larger piece of tinfoil to reduce the risk of contamination.

2.2.11 Radiometric dating of sediment cores

The Radiometric dating referred to in this thesis were preformed by NIRAS in 2019/2020, where the samples mentioned in Ekeroth et al., 2020, were sent to the Gamma Dating Center at the Institute of Geography, University of Copenhagen, Denmark. The radiometric dating is based on ^{137}Cs, ^{210}Pb and ^{226}Ra. The measurements were carried out on a Canberra ultralow-background Ge-detector.

2.3 Plastic analysis

The microplastics extracted from the samples according to the methods used in the section above, were identified with the procedure used at the Norwegian Institute for Water Research (Lusher, 2020).

2.3.1 Visual observation

Filter papers used to filtrate samples in the laboratory for freshwater filtration and density separation were inspected (four filter papers per sample). It was important that the filter papers were completely dry before visual analysis, to be able to differentiate between textures for plastic and non-plastic particles.

NIVA suggested several methods for isolating the plastic particles in the visual observation stage. One of the three approaches were used in this thesis. One way were to transverse the filter paper in a logical order. The principle of the method used in this process was to transverse the filter paper systematically, picking all particles $> 50\mu m$, suspected to be plastic, with the help of pointy tweezers. The particles were then placed around the brim of the filter paper, in groups with similar particles (Fig 2.9).

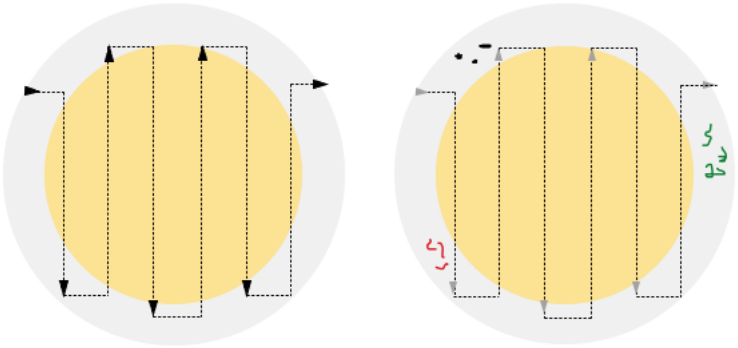

Figure 2.9: Illustration of the picking process, inspired by (Lusher, 2020).

2.3.2 Characteristics and measurements

Every picked particle were characterized in respect to color, size and shape. Each particle was named, by sample number and particle number, with descriptions of the particle, color and length of the longest and the shortest axis. The date of characterisation is also included, as well as comments if unusual textures or shine is observed (Appendix B, Table B.1).

2.4 Classification of microplastic

To obtain the microplastic-type, Raman- and Fourier Transform Infrared (FTIR) spectroscopy were used. Both methods are relatively fast and able to provide enough chemical information to disclose the type of plastic the samples most probably are composed of.

2.4.1 Raman spectroscopy - Theory

Raman spectroscopy is a method by which vibrational characteristics of a sample is measured indirectly via inelastic scattering of monochromatic light (Fig. 2.10). When monochromatic light (laser light) is directed onto the sample, parts of the light will be absorbed, transmitted, reflected and scattered, simultaneously. Raman spectroscope is solely interested in the part of scattered light that has lost energy corresponding to the vibrational states that characterize the sample. However, the major part of scattered light, is Rayleigh scattering, where no energy loss has occurred. The probability that a photon loses energy and becomes a Raman photon is about one to ten million Rayleigh photons - so the Raman effect is quite weak. Figure 2.11 show the differences between Rayleigh, Raman and Anti-Stokes scattering. Anti-Stokes scatter can be removed by using a long-pass filter. The Raman spectrometer used in this analysis, a *Horiba Jobin-Yvon T64000*, can be found at the third floor in the Chemistry building, UiO.

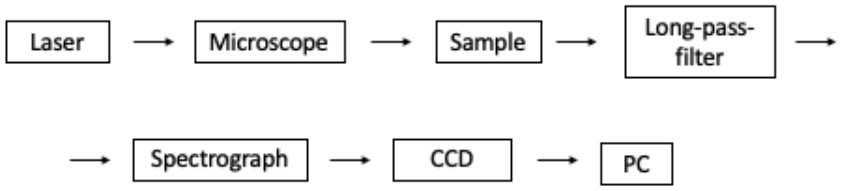

Figure 2.10: Schematic representation of a Raman spectrometer.Inspired by (Siesler and Holland-Moritz, 1980).

2.4.2 Raman procedure

Paracetamol was used as a reference compound, and was measured twice during the day, to enable offsets and scale errors that are common for dispersive spectrographs. The filter papers were removed from the petri-dishes in this step of the analysis, this to prevent the plastic in the petri-dish to be detected in the spectrum representing the analysed particle. The filter paper was transferred to a glass slide under the microscope, and white light were used for visible observation. The particle was then found by using a camera connected to the microscope, before adjusting the focal-point and observation of the laser point on the particle surface. A running exposure measurement was done to perform a final optimization of all settings before launching the final measurement. Before the Raman could be performed, all lights and the computer screen had to

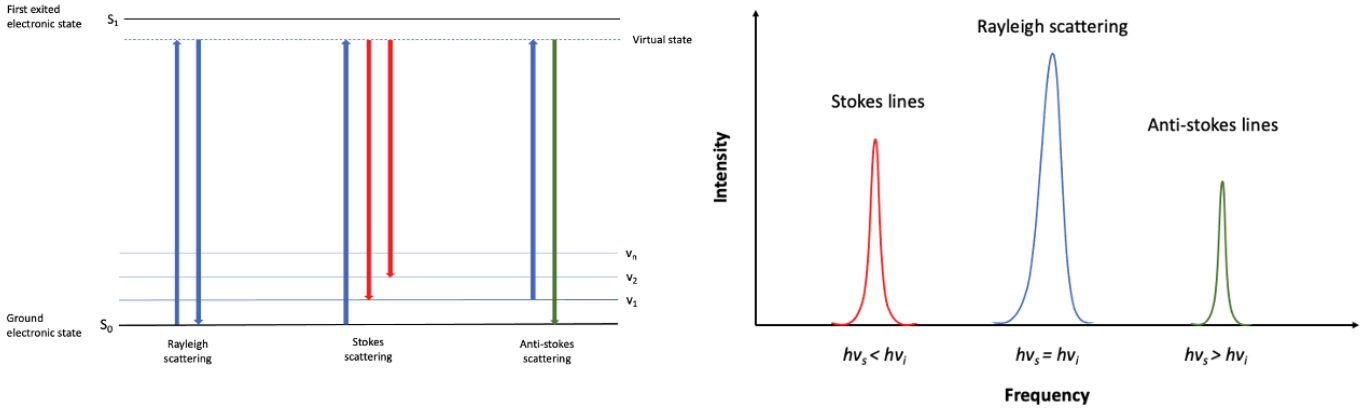

Figure 2.11: The principle of Rayleigh, Stokes, and Anti-stokes scattering schematically illustrated (Modified after (TracesCentre, 2021)).

be shut off (Fig. 2.12). To prevent destruction of the sample, the laser was damped to 400 µW at the sample. The laser used in the Raman spectroscopy had a wavelength of 532.1 nm. The acquisition time was chosen based on the observed fluorescence level, in order to avoid saturation of the detector.

Each spectrum was saved before treated, to reduce background noise for further analyses. The spectrum was corrected with a polygon function to reduce the background noise and fluorescence of the sample. The spectrums were also scale corrected by linear interpolation of paracetamol peaks.

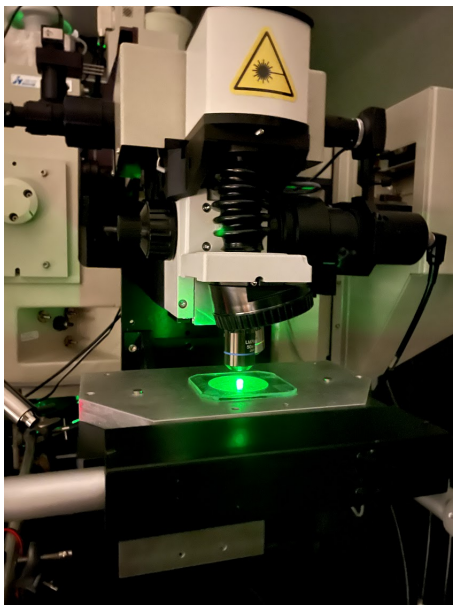

Figure 2.12: Raman spectroscopy of HDPE (high-density polyethylene) test particle, provided by NIVA, illuminated by a 532.1 nm green laser.

The Raman spectra for the tested material were sent to Post Doctoral Researcher, Sebastian Primpke at the Alfred Wagner Institute, Germany, for further analysis and identification. Databases used for identification were: AWIMaterials-Witec, Cabernard et al, ELi, HAnordanisch, HC-Verbindungen, HFarbstoffe, HPolymere, HSI-Verbindungen, Oliver, SLOPP and SLoPP-E.

2.4.3 ATR-FTIR - Attenuated total reflection Infrared spectroscopy - Theory

In addition to visual analysis of microplastic, a few particles of each group of visually equal particles were further analysed by Fourier-transform infrared spectroscopy (Fig. 2.13). The FTIR machine was added an Attenuated total reflection cell, where the light is transitioned through the sample (Fig.2.14). By using FTIR to determine the chemical properties of the particle, the results were complimentary to the Raman analysis. A disadvantage of using FTIR was that the particles could be destroyed, and therefor not be tested twice. The ATR-FTIR spectrometer, *SHIMADZU IRPrestige-21*, can be found at the second floor in the Chemistry building, UiO.

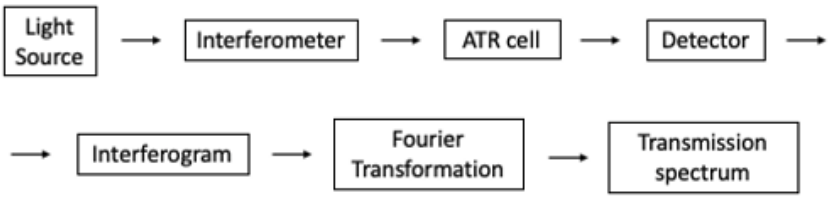

Figure 2.13: Schematic representation of an FTIR spectrometer, where the sample chamber is specified by the ATR-FTIR procedure. The ATR cell is a supplement for the FTIR spectrometer. Inspired by (Siesler and Holland-Moritz, 1980).

An ATR cell (Attenuated total reflection cell) was added to the Fourier-transform infrared spectroscopy. Without the ATR cell, the light is transitioned through the sample, instead of reflected off of the sample. ATR works via total internal reflection within a diamond crystal. However, a small portion of the reflected light forms a wave at the diamond surface (the evanecent wave). If parts of this wave is absorbed by the sample pressed onto the diamond a decrease in total reflection occurs. The absorbed infrared light discloses the chemical composition of the sample, which can be read by the produced spectrum.

2.4.4 FT-IR procedure

The FTIR measurements started with running a background measurement, where $CO_2(g)$ and $H_2O(g)$ were observed. The background spectra was measured using the clean ATR cell alone. The microplastic was then carefully transferred from the filter paper to the diamond crystal. Before running the FTIR, the particle was squeezed slightly by screwing the pressure tower carefully, this was done to make the surface of the particle larger for better optical

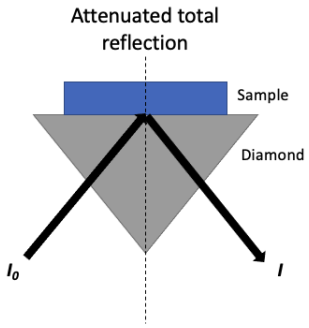

Figure 2.14: Principle of ATR-IR with total reflection.$IandI_0$ is the intensity of the light onto the sample and transmitted or reflected by the sample. Modified from (Bürgi, 2011).

contact between the particle and the diamond cell (Fig. 2.15). Each spectrum was average of 128 scans, both for the background and for the microplastic measurements, which took approximately 5 minutes. After the analysis the spectre was saved, and the diamond and pressure tower were cleaned and prepared for the next sample.

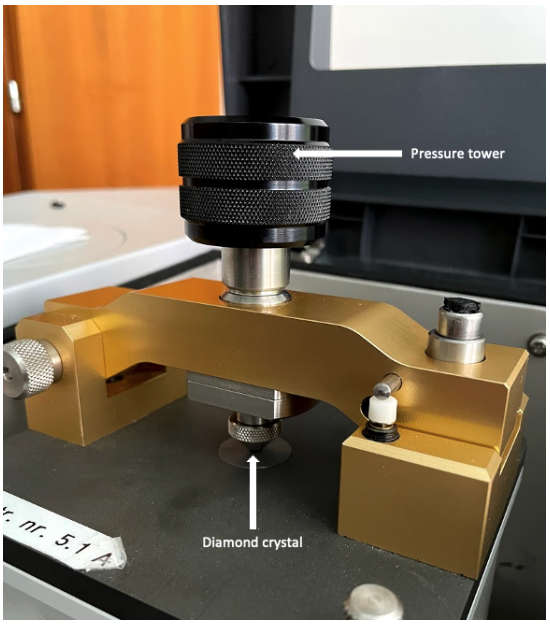

Figure 2.15: ATR-FTIR spectroscopy of microplastic, squeezed onto the diamond with the pressure tower.

The ATR-FTIR spectra were also sent to Post Doctoral Researcher Sebastian Pimpke at the Alfred Wagner institute, Germany, for further analysis.

3 Results

3.1 Collected CTD-data

The collected CTD data for the water column, conductivity (salinity), temperature and pressure/density, are presented in figure 3.1. The oxygen content of the water column shows similar concentration for both sampling sites, with a decrease downwards. The concentration of oxygen in the water column varies in the upper part, from 6.5-12.5 mg/L, before stabilizing around 2 mg/L at approximately 60 meters water depth.

For the temperature data, the temperature remains stable (at app. 17°C) in the upper 5 meters of the water column, before decreasing down to 25 meters water depth. The temperature again becomes stable at approximately 7°C form 25 to 80 meters, where the sediment core was collected.

The salinity of the water column at the two sampling sites increases downwards. Where the salinity remains relatively stable around 1 PSU, in the first 5 meters. The salinity then increase rapidly in the interval 5 to 10 meters water depth, before reaching a new point of stabilization (salinity app. 30 PSU) at approximately 25 meters water depth.

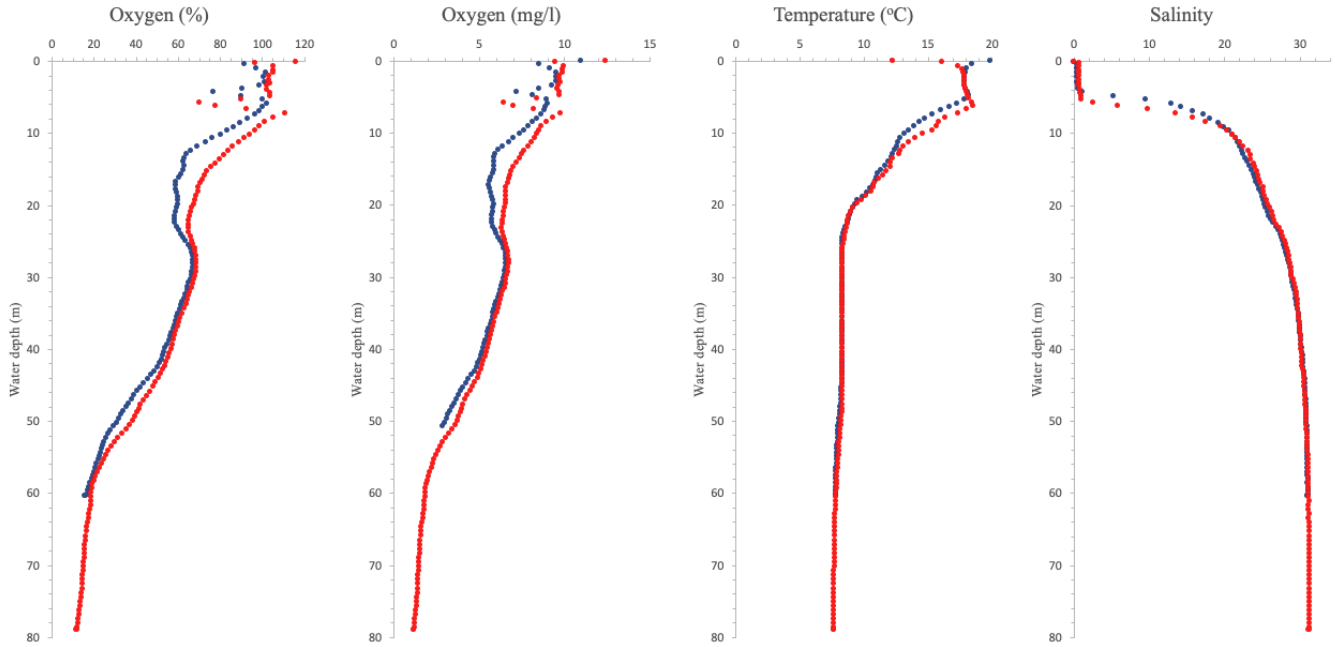

Figure 3.1: Collected CTD-data for the water column, at the locations DRA1 (Blue) and DRA2 (Red) in Drammensfjorden.

3.2 Sediment cores - log and description

3.2.1 DRA2A

The sediment core collected, measured a length of 63 cm, where the upper 50.5 cm of the sediment were sampled for microplastic analysis. Visual observations of the core showed higher density of the sediment down core. The sediment core had a clear lamination (Fig. 3.2), with little bioturbation, as well as shell and rock fragments throughout the core. What could look like bioturbation were be observed down to 12 cm depth. The layering of the sediment pack varied in colors from light gray to black, and in thickness from less than a millimeter to approximately 3 mm. The majority of the sediment could be described as clay to fine clay, with two coarser fine-sand layers around 40 and 50 cm depth. There were also observed oxidation of the sediment during subsampling (Tab 3.1). Detailed sediment log for 5BxE is provided in Appendix A, Figure A.1.

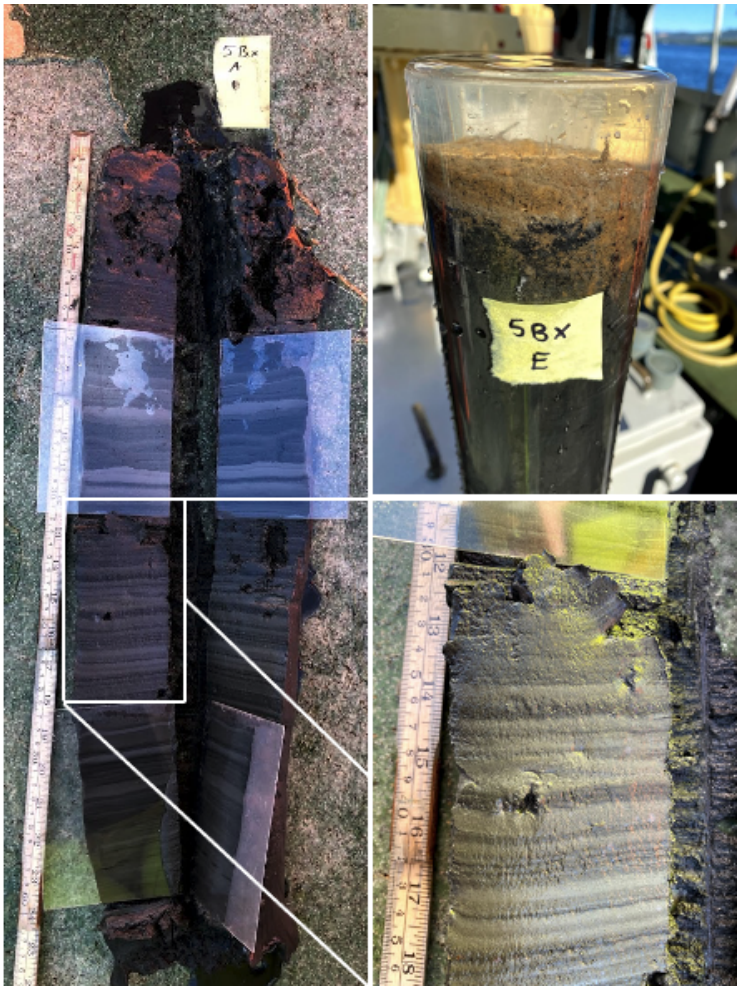

Figure 3.2: Sediment cores collected at location DRA2A, where 5BxA was logged and 5BxE was described and sampled.

Table 3.1: Sediment core description scheme, core 5BxE/DRA2A.

Station and core name:	Water depth (m):	Latitude:	Longditude:
5BxE/DRA2A	**80 m**	**010°17.484'**	**59°43.003'**

Sediment surface observations:	Core length:	Sampling device:
Bioturbation, brown surface	**63 cm**	**Gemini twin corer**

Date: 25.08.2020 **Weather conditions:** Sunny, slightly windy, 17°C

Core depth (cm)	Color	Treatment	Comments
0-1	Dark gray to black	Freezdryer	Bioturbation, black areas in a dark gray matrix, some brown surface sediment (org.material)
1-2	Dark gray to black	Freezdryer	Less black areas in the dark gray matrix
2-3	Dark gray to black	Freezdryer	Black areas in a dark matrix
3-4	Dark gray	Freezdryer	Shell, more dense sediment
4-5	Dark gray with black spots	Freezdryer	Denser sediment
5-6	Dark gray with black spots	Freezdryer	Bioturbation or gas (voids)
6-7	Dark gray almost blackish	Freezdryer	Voids
7-8	Dark gray almost blackish	Freezdryer	Voids, sediments more black than gray
8-9	Black with gray areas	Freezdryer	Voids, mostly black
9-10	Black with gray areas	Freezdryer	Voids
10-11	Black with gray areas	Freezdryer	Voids
11-12	Dark gray	Freezdryer	Voids, very dense sediments
12-13	Dark gray with lighter gray areas	Freezdryer	Voids, probably from escaping gas
13-14	Dark gray with light gray and black spots	Freezdryer	Voids
14-15	Dark gray with light gray and black spots	Freezdryer	Voids
15-16	Dark gray with smaller black areas	Freezdryer	Voids
16-17	Dark gray with black spots	Freezdryer	Less voids
17-18	Lighter gray with dark gray areas	Freezdryer	Few voids
18-19	Dark gray with lighter gray areas	Freezdryer	No voids
19-20	Homogeneous dark gray	Freezdryer	-
20-22	Gray with darker gray spots	Freezdryer	-
22-24	Dark gray with black areas	Freezdryer	-

Core depth (cm)	Color	Treatment	Comments
24-26	Dark gray with black areas	Freezdryer	Some light gray spots
26-28	Gray with darker gray areas	Freezdryer	-
28-30	Gray to dark gray	Freezdryer	-
30-32	Dark gray with black areas	Freezdryer	Less voids
32-34	Dark gray	Freezdryer	Some lighter gray and black areas
34-36	Gray to dark gray	Freezdryer	Black areas
36-38	Gray to light gray	Freezdryer	Lighter in color
38-40	Light gray	Freezdryer	Darker gray around the edges, might be due to oxidation
40-44	Light gray	Freezdryer	Oxidation
44-48	Homogeneous light gray	Freezdryer	Very homogeneous mass
48-50.5	Light gray	Freezdryer	Very homogeneous mass

3.2.2 DRA2B

The sediment core measured a length of 62 cm, where 51 cm of the sediment were sampled for microplastic analysis. The stratigraphy of the sedimentation was similar to the layering of core DRA2A. The two cores were collected in the same deployment of the Gemini-twin-corer. The core contained more fragments of bryosos and shells, than core DRA2A. Detailed sediment core description is provided in Appendix A, Table A.1.

3.3 Water content

The graphs in Figure 3.2 illustrates the water content of the two cores, with a downward decrease of water in the sediment (Tab A.2 and A.3). The two sediment cores show similar percentage of water throughout the core. The water content close to the seafloor contains larger amounts of water than down core, where the fist 5 cm has an almost linear decrease from 85 to 60%. For the following 10 cm, the content of water remains stable between 60 and 65%. A sudden change in the water content can be observed for both cores at approximately 15-20 cm depth, where the water content changes from around 60 to 45%.

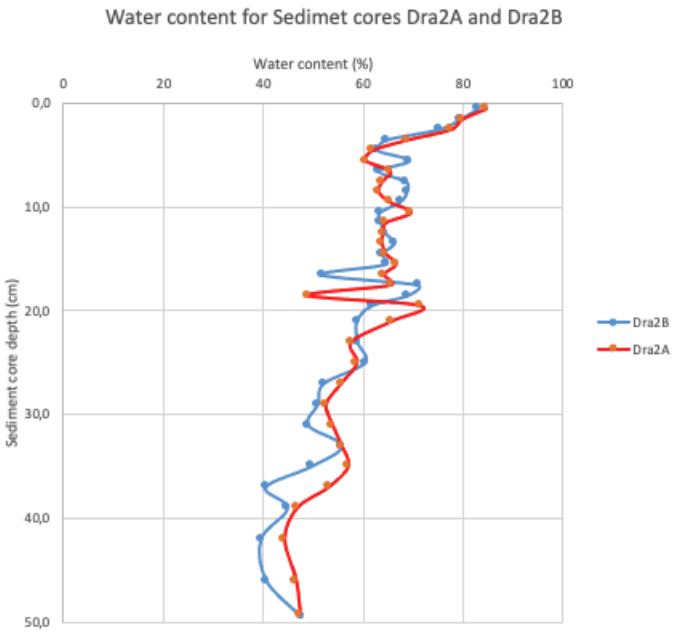

Figure 3.3: Water content, calculated by weight, for the two sediment cores collected at station DRA2, named DRA2A and DRA2B.

3.4 Sediment dating - NIRAS

The sediment cores collected were dated based on the sediment collection of NIRAS in 2019 (Ekeroth et al., 2020).

The upper 30 cm of the sediment cores, according to Ekeroth et al., 2020, dates back to 1922. The highest accumulation rates where in the years 1966-1977 and around 2012, with an accumulation rate of 1.9 ($kgm^{-2}y^{-1}$).

Table 3.2: Chronology and accumulation of sediment for the location 5B, based on radiometric dating of ^{137}Cs and ^{210}Pb, from Ekeroth et al., 2020.

Sediment depth (cm)	Age (y)	Margin of error (y)	Year	Accumulation rate ($kgm^{-2}y^{-1}$)	Margin of error ($kgm^{-2}y^{-1}$).
0			2019		
0.5	0	1	2019	1.4	0.17
1.5	2	1	2017	1.4	0.14
2.5	3	1	2016	1.6	0.26
4.5	7	2	2012	1.9	0.19
6.5	14	2	2005	1.3	0.15
8.5	21	2	1998	1.3	0.21
10.5	26	2	1993	1.7	0.20
11.5	30	2	1989	1.2	0.19
12.5	33	2	1986	1.8	0.37
13.5	36	2	1983	1.4	0.23
14.5	40	2	1979	1.4	0.60
15.5	42	2	1977	1.9	0.43
18.5	50	3	1969	1.9	0.58
20.5	53	3	1966	1.9	0.34
22.5	59	3	1960	1.5	0.35
24.5	66	3	1953	1.6	0.22
26.5	75	2	1944	1.2	0.21
29.5	97	2	1922	0.9	0.37

3.5 Microplastic in sediment cores

Microplastic found in the sediment core DRA2A at station DRA2 were counted and described, before visualised in Figure 3.4. The visualisation of observed microplastic, was calculated based on tables in appendix B.

3.5.1 Microplastic count

There were picked 1361 particles in total, with an average of 45,3 particles per slice. The microplastic count per gram dry sediment were calculated for core DRA2A (table B.4), the total weight of the dry sediment was 904.057 grams, which makes the average microplastic/gram dry sediment 1.505 (Table. 3.3).

Microplastic picked and observed throughout the core can be seen graphically in figure 3.4a. Particles smaller than 50µm were not taken into account. Fragile green glitter fragments, smaller than 50µm, were observed at several depths in the sediment core. The accumulation of plastic particles have an increasing trend in particle count form the sediment surface until about 8-9 cm depth. The highest accumulation of plastic particles can be seen from 8-11 cm depth, before observing a decreasing trend in microplastic accumulation downwards in the core. A slight increase in plastic particles can be observed between 19-30 cm.

Table 3.3: Microplastic per gram sediment in sediment core DRA2A.

DRA2A	Microplastic	Sediment weight (g)
Total	1361	904.057
Average (MP/g)	**1.505**	

3.5.2 Color

Picked microplastic were divided into color categories, black, brown, gray, white, transparent, blue, red, green and yellow. The distribution of colored particles can be seen in figure 3.4b. The majority of plastic particles picked are of darker colors, mostly black and brown. The accumulation of colored particles (red, blue, green and yellow) can be observed from 5-15cm core depth. The dark colored particles decrease in number from the upper core until 8 cm, before increasing. White particles can be observed in larger numbers between 6 and 11 cm depth and down core from 32 cm depth. For the distribution of colored particles, the highest concentration can be observed around 4-5 cm depth, where green particles account for the majority of picked particles at this depth (Fig.3.5.).

Table 3.4: Color distribution in core DRA2A.

	Black	Brown	White	Gray	Transparent	Red	Blue	Green	Yellow
Distribution (%)	64.5	5.6	15.9	3.7	0.9	1.0	0.6	6.3	1.5

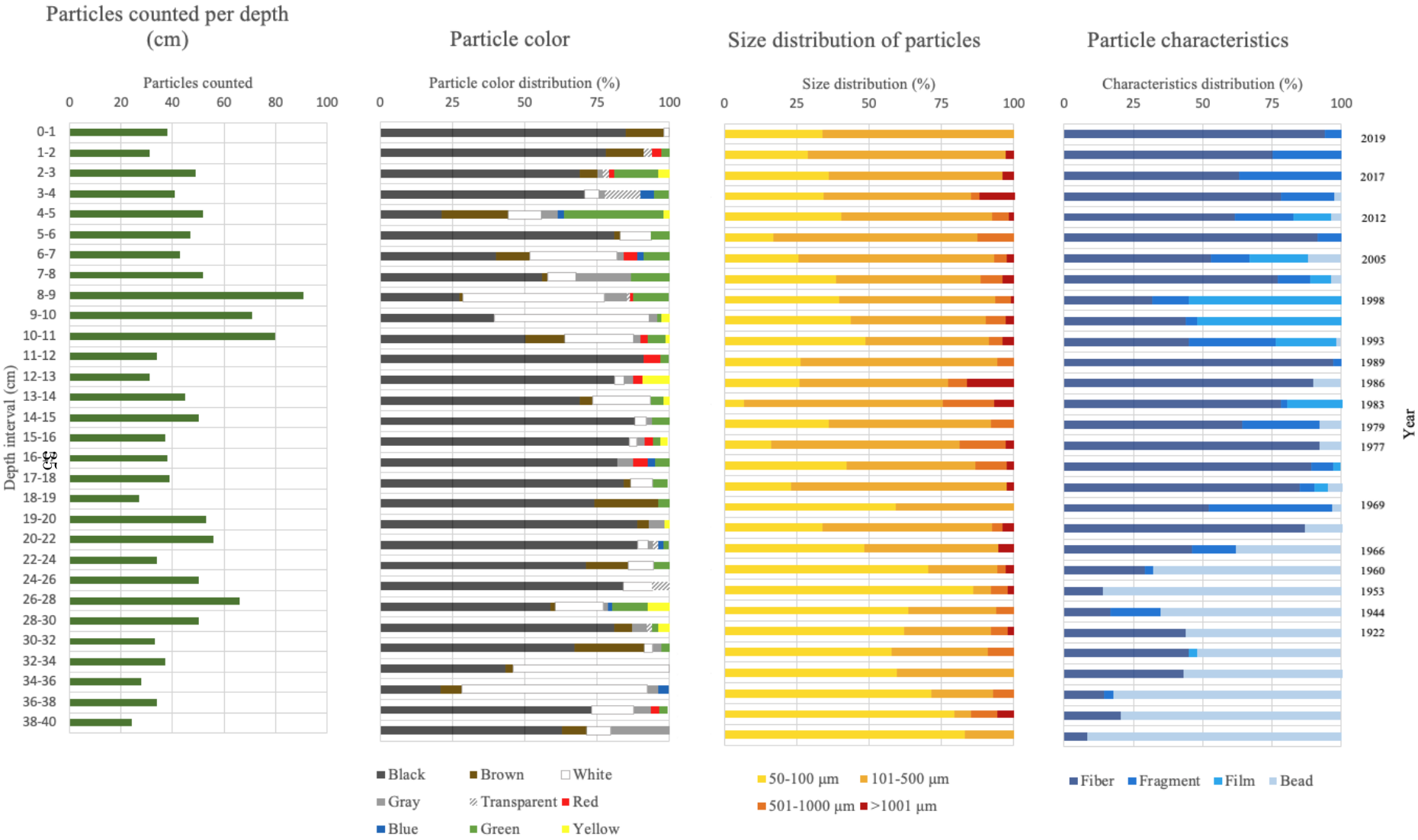

Figure 3.4: Visual data presented in graphs, **a.**Particle count per sediment depth. **b.** Color distribution per sediment depth. **c.**Size distribution per sediment depth. **d.**Particle characteristics (shape) per sediment depth.

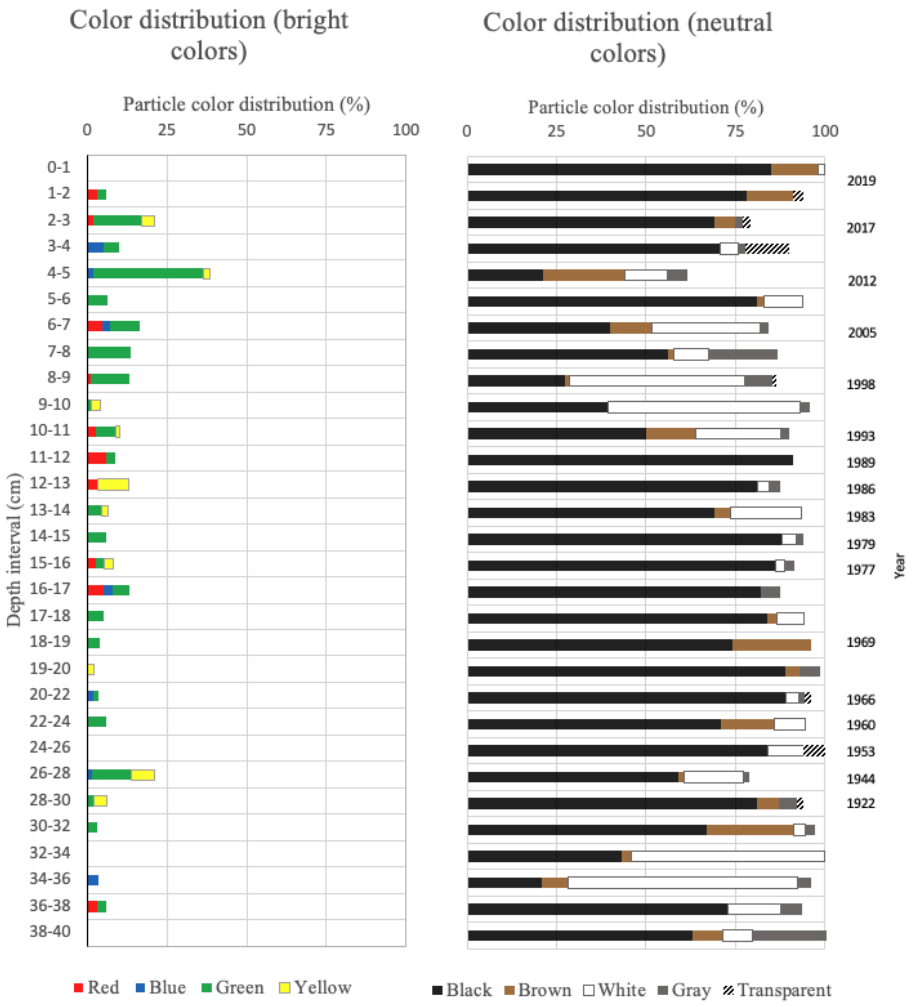

Figure 3.5: Color distribution of particles in core DRA2A. **a.** Distribution of bright colored particles. **b.** Distribution of neutral colored particles.

3.5.3 Particle size

The particle size distribution was divided into several groups where the smallest interval measured 50-100µm, second interval measured 101-500µm, third interval measured 501-1000µm. Particles larger than 1001µm were characterized as its own group >1001µm. Small and mid-range sized particles dominated the observed plastic. A slight shift can be observed from 20 cm and down throughout the core, where particles in the size 50-100 µm counts for more than 50% of the picked particles (Fig. 3.4.c).

Table 3.5: Distribution of microplastic from core DRA2A, according to shape.

	50-100µm	101-500 µm	501-1000 µm	>1000 µm
Percentage	43.3	48.1	5.8	2.9

3.5.4 Shape

The distribution of shapes in the picked material were divided into four categories; fibers, fragments, films and beads. The upper core consists mostly of fibers, there can also be observed a shift in shape around 8 cm, where film particles are more present. A second shift can be seen from around 20 cm and downwards, where the majority of the particles observed are beads (Fig.3.4.d).

Table 3.6: Distribution of microplastic from core DRA2A, according to shape.

	Fiber	Fragment	Film	Bead	Total
Total	765	159	138	300	1361
Percentage	56	11	10	23	100

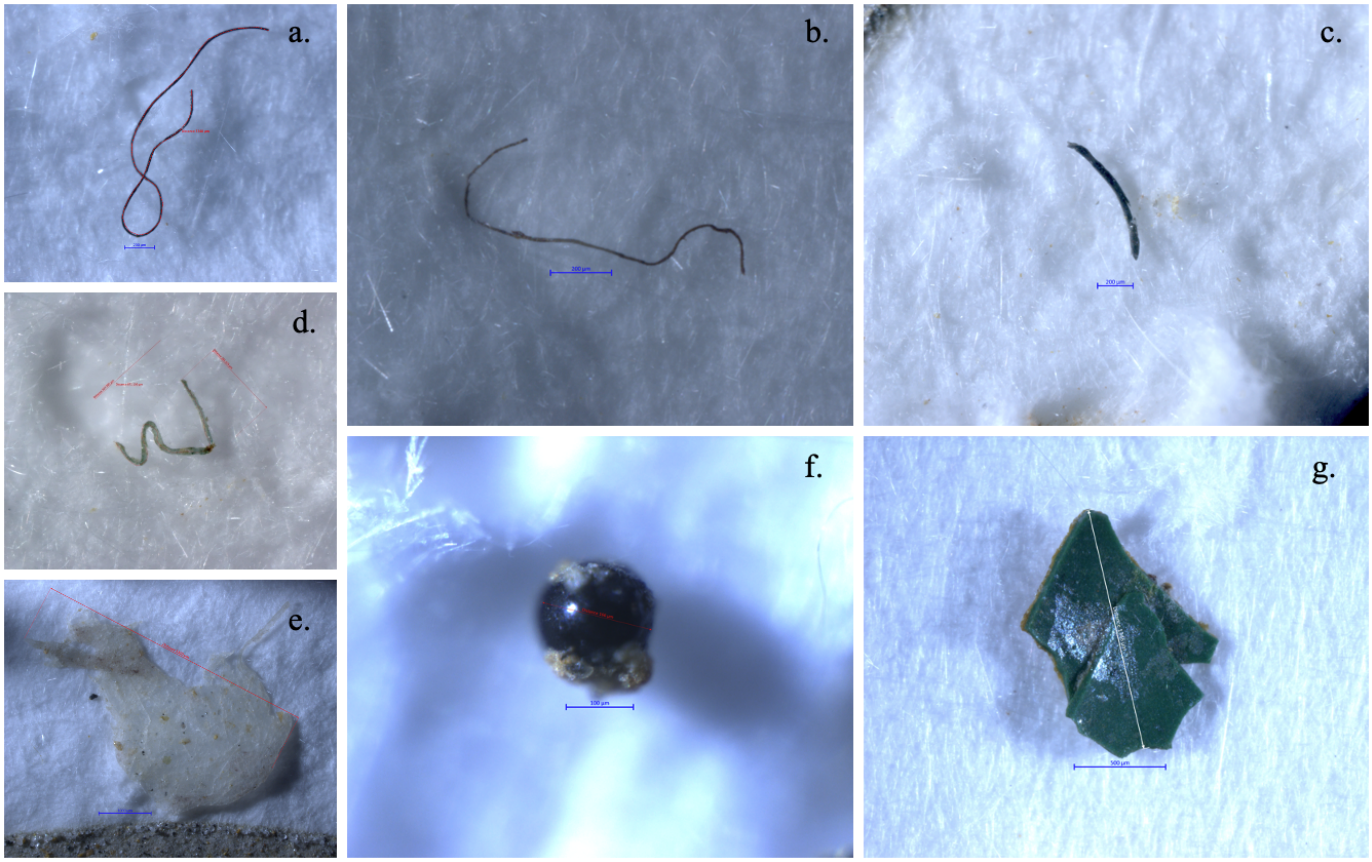

Figure 3.6: Photo of microplastic found in sediment core DRA2A. Larger figures with scale in Appendix C. **a.** Black fiber from sample DRA2A.2-3.1 (scale 200µm). **b.** Gray/Brown fiber from sample DRA2A.16-17.3 (scale 200 µm). **c.** Blue fiber from sample DRA2A.3-4.1 (scale 200 µm). **d.** Green fiber from sample DRA2A.16-17.3. **e.** White film from sample DRA2A.20-22.2 (scale 1000 µm). **f.** Black bead from sample DRA2A.38-40.3 (scale 100 µm). **g.** Green fragment from sample DRA2A.26-28.3 (scale 500 µm).

3.6 Raman data

24 out of the 1361 picked particles were tested by Raman spectroscopy, only seven particles were identified. Four out of the seven particles identified, were determined to be plastic. Identified types that may indicate plastic, were polyethylene and anthrophogenic pigment (Table 3.5).

3.7 FT-IR data

16 out of the 1361 picked particles in core DRA2A were tested by FTIR, only 6 particles were identified. The Identified particles came back as; Anthropogenic pigment, Silicon rubber and black carbon (Table 3.6), black carbon does not classify as plastic or polymer.

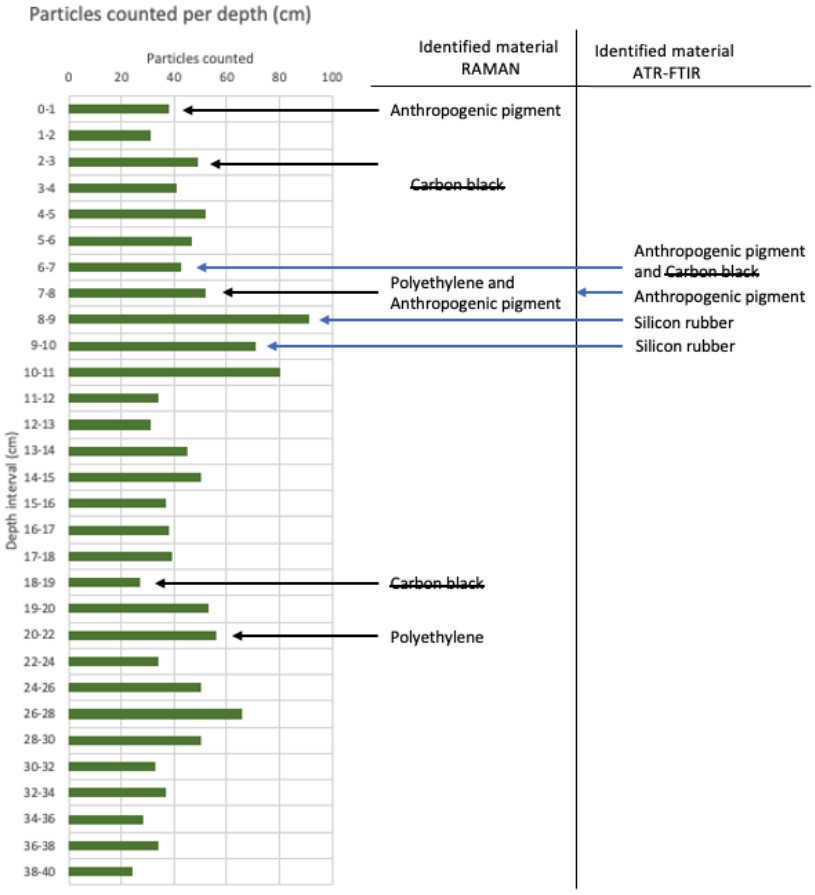

Figure 3.7: Overview of identified particles at specific depths. Non-plastic and pigment particles included.

Table 3.7: Particles extracted from core DRA2A collected from Drammen in August 2020. Data is displayed as particles per depth interval (cm) and particles are described based on their visual characteristics (Lusher, 2020) and chemical profiles obtained by Raman spectroscopy.

Depth interval (cm)	Sample name	Particle description	**Expert evaluation**
0-1	DRA2A.0-1.4	Black fiber	Not identified
0-1	DRA2A.0-1.4	Black fiber	Anthrophogenic pigment
2-3	DRA2A.2-3.4	Black and white fragment	Not identified
2-3	DRA2A.2-3.4	Black fiber	Not identified
2-3	DRA2A.2-3.4	Black fiber	Carbon black
2-3	DRA2A.2-3.4	Black fiber	Not identified
5-6	DRA2A.5-6.3	Black fiber	Not identified
5-6	DRA2A.5-6.3	Black fiber	Not identified
5-6	DRA2A.5-6.3	Black fiber	Not identified
5-6	DRA2A.5-6.3	Black fiber	Not identified
5-6	DRA2A.5-6.3	Black fiber	Not identified
7-8	DRA2A.7-8.2	Blue fiber	Polyethylene
7-8	DRA2A.7-8.2	Green fiber	Not identified
7-8	DRA2A.7-8.2	Green fiber	Anthrophogenic pigment
7-8	DRA2A.7-8.2	White film	Not identified
13-14	DRA2A.13-14.3	Black fiber	Not identified
13-14	DRA2A.13-14.3	Black fiber	Not identified
13-14	DRA2A.13-14.3	Black fiber	Not identified
13-14	DRA2A.13-14.3	Mineral	Not identified
13-14	DRA2A.13-14.4	White fiber	Not identified
18-19	DRA2A.18-19.4	Black fragment	Carbon black
20-22	DRA2A.20-22.4	White film	Not identified
20-22	DRA2A.20-22.4	Black fiber	Not identified
20-22	DRA2A.20-22.4	White film	Polyethylene
26-28	DRA2A.26-28.4	Green fragment	Not identified

Table 3.8: Particles extracted from core DRA2A collected from Drammen in August 2020. Data is displayed as particles per depth interval (cm) and particles are described based on their visual characteristics (Lusher, 2020) and chemical profiles obtained by ATR-FTIR spectroscopy.

Depth interval (cm)	Sample name	Particle description	**Expert evaluation**
6-7	DRA2A.6-7.2	Blue fiber	Anthrophogenic pigment
6-7	DRA2A.6-7.4	Red and Black fragment	Not identified
6-7	DRA2A.6-7.4	Black fiber	Carbon black
6-7	DRA2A.6-7.4	Black fiber	Not identifiable
7-8	DRA2A.7-8.4	Red fiber	Not identifiable
7-8	DRA2A.7-8.4	Yellow fiber	Anthrophogenic pigment
8-9	DRA2A.8-9.3	White film	Silicon rubber
9-10	DRA2A.9-10.2	White film	Silicon rubber
9-10	DRA2A.9-10.2	White bead	Silicon rubber
12-13	DRA2A.12-13.2	Green fragment	Not identified
12-13	DRA2A.12-13.2	White film	Not identified
12-13	DRA2A.12-13.3	Black fiber	Not identified
15-16	DRA2A.15-16.1	Black fiber	Not identifiable
15-16	DRA2A.15-16.1	white fiber	Not identifiable
15-16	DRA2A.15-16.1	Blue fiber	Not identifiable

3.8 Blank-tests

Blank-tests taken during subsampling of the sediment cores show some contamination of fibers. 16 and 10 fibers were detected in sample 5BXE and 5BXF during subsampling of core DRA2A and DRA2B, the majority of there particles were black and blue.

For the blank-test of filtered water used for cleaning the sampling boxes, 4 particles were detected.

Table 3.9: Summary of particles found in blank-samples of filtered water, and taken during sampling of sediment cores. **Blank1** sample of filtered water for cleaning, **5BXE** and **5BXF** contamination samples during subsampling of cores *DRA2A* and *DRA2B*, while **DH1A** and **DH1H** contamination samples during subsampling of cores *DRA1A* and *DRA1B*. Blant-tests analysed by Amy Lusher at NIVA.

Sample	Total	Red	Blue	Black	Gray	Clear
Blank1	4	2	1	0	1	0
5BXE	16	1	7	8	0	0
DH1A*	19	3	8	7	1	0
5BXF	3	0	1	1	0	1
DH1H*	10	1	6	3	0	0

*DH1A and DH1H are blank-samples taken during sampling of DRA1A and DRA1B, which are sediment cores used in Thorstensen, 2021.

4 Discussion

4.1 Sample preparation - comments

The use of hydrogen peroxide in removing the organic material, is of limited efficiency (Mikutta et al., 2005). Depending on the particle size, between 12 and 93% organic matter is typically removed. Mikutta et al., 2005 also points out that a pH range between 6 and 7.5 is most efficient. It is therefore uncertain how well the removal of organic material in the samples were. The efficiency of the organic material removal could have been tested by using test samples of sediment. The organic material removal could be decided by calculated the total mass loss, that can be assumed to directlu reflect the loss of organic material in the sample. The total mass loss can therfore be used to estimate the percentage of organic material removal (R. R. Hurley et al., 2018).

Since the efficiency of the organic material removal is unknown, it is possible to mistake plastic particles covered in organic material or carbon, for coal fragments or non-plastic particles, as can be seen in the Raman spectrum. Fibers that are visually observed as plastic may have spectra indicating organic material or carbon as in coal, but can not be neglected as possible plastic particles until proven otherwise, as it can be either organic coating of plastic particles or organic particles mistaken for plastic.

The hydrogen peroxide can also cause problems with the Sodium iodide, where residual of hydrogen peroxide can oxidize the iodide, $I \longrightarrow I_2$. The oxidized iodide can then react with remaining iodide and produce tri-iodide $H_2O_2 + 2H^+ + 3I^- \rightleftharpoons 2H_2O_2 + I_3^-$ (Johnson and Myers, 1996). The Raman spectrum for tri-iodide has a significant top around 110 cm^{-1} for the Raman shift. This can therefore explain the Raman spectra for some of the particles, where the significant top lays at lower frequencies than 200 cm^{-1}. Tri-iodide and free iodine might therefore exist in the samples treated this way.

By repeating the freshwater filtration step several times in the preparation process, the risk of hydrogen peroxide oxidising the iodide would decrease, and the tri-iodide would not be as present in the solution. Another approach of the issue is to use a septic tank cleaner to remove the organic material . This method can reduce the organic material in the sample by 93%, and possibly remove the cause of oxidation of iodide (Lavoy and Crossman, 2021).

The density separation liquid can also be changed to reduce or remove the risk of oxidation between hydrogen peroxide and iodide. Na_2WO_4 can be used as an alternative to the NaI solution, but was to expensive to use in this matter.

The most commonly used solutions for density separation are listed in Table 4.1 and densities for common plastic types in table 4.2. The sodium iodide solution has a higher density than most commonly used solution, and is therefore more efficient in separating higher density polymers from the samples (Frias et al., 2018).

Table 4.1: Commonly used density separation solutions. Modified from Frias et al., 2018.

Chemical formula	Reagent name	Density solution (gcm^{-3})	Health hazard (Toxicity*)	Average price (€per 250g) †	Safety-Price Index
NaCl	Sodium chloride	1.0-1.2	1 (low)	3	green
$Na_2WO_4 \cdot 2H_2O$	Sodium tungstate dihydrate	1.40	2 (low)	70	green
NaBr	Sodium bromide	1.37-1.40	2 (low)	3-5/430 §	green
$3Na_2WO_4 \cdot 9WO_3 \cdot H_2O$	Sodium polytungstate	1.40	2 (low)	276	red
$Li_6(H_2W_{12}O_{40})$	Lithium metatungstate	1.60	1 (moderate)	360 ‡	red
$ZnCl_2$	Zinc chloride	1.6-1.8	3 (high)	45	red
$ZnBr_2$	Zinc bromide	1.71	2 (high)	200	red
NaI	Sodium iodide	1.80	2 (moderate)	130	yellow

*Health hazard retrieved from NFPA/HIMS forms and toxicity values from MSDS; †quotes for Ireland dated from March 2018,**please note that price values may vary in other countries;** §The cost of Sodium bromide (NaBr) is one example of the price fluctuation between countries - in Germany is very cheap (green) and in Ireland is extreamly expensive (red) which drastically affect the Safety price Index ‡Lithium metatungstate quotes only available for a volume of 250 ml.

Table 4.2: Common polymer densities. Polymers below the green line can't be separated bu using NaCl as a density separation solution, and polymers below the purple line cant be separated by any of the solutions mentioned in table 4.1. Modified from Enders et al., 2015; Frias et al., 2018.

Abbreviation	Polymer	Density (gcm^{-3})
PS	Polystyrene	0.01-1.06
PP	Polypropylene	0.85-0.92
LDPE	Low density polyethylene	0.89-0.93
EVA	Ethylene Vinyl Acetate	0.94-0.95
HDPE	Hight dencity polyethylene	0.94-0.98
PA	Polyamide	1.12-1.15
PA 6,6	Nylon 6,6	1.13-1.15
PMMA	Poly metyl methacrylate	1.16-1.20
PC	Polycarbonate	1.20-1.22
PU	Polyurethane	1.20-1.26
PET	Polyethylene terepthalate	1.38-1.41
PVC	Polyvinyl chloride	1.38-1.41
PTFE	Polytetrafluoroethylene	2.10-2.30

Polymers until the marked lines are retained by the solutions. Please note that this is a theoretical model and some polymers with higher densities could potentially be found in sediments even using a solution with density lower to 1.40 g cm-3 .

4.2 Evolution of microplastic pollution in Drammen

Industrial activity in the area of Drammen may be a contributor to plastic pollution into the fjord. As mentioned in section 1.2.3, the city of Drammen has a industrial history including many possible sources of plastic pollution into the fjord.

Looking at the historical events in perceptive of plastic waste and evolution, and comparing to observed changes in microplastic in the sediment, there is no clear change in counted microplastic with the occurrence of new polymers introduced into the market. On the other hand, there is a clear correlation between establishment of treatment plants and decreasing accumulation of observed particles in the sediment core collected (Fig.4.1).

Due to the lack of identified microplastic, it is difficult to determine the exact source of contamination, and also to determine the individual impact of the different plastic production events.

The change in microplastic count seen in a industrial perspective show little to no correlation between plastic production start and the amount of particles found in the sediment. The change in microplastic shape and size distribution on the other hand, appears to have a direct correlation, with an acceleration of the plastic production in mid- to late 1960's (Fig. 4.2). The main shape of microplastic observed down core were beads, while after the explosion in plastic manufacturing during the 1960's, the majority of observed particles were fibers. At the same time, there were a significant change in size, from smaller (50-100 µm) to larger particles (50-500 µm).

Figure 4.1 indicates occurrence of microplastic in the sediments before known plastic industry. There may be more than one answer to the question "why"?

1. The observed material may not be plastic.
2. Bioturbation or disturbance in the sediment can cause mixing of old and new sediment.
3. The use of natural rubber started earlier than the commercial production of rubber.

Another major factor contributing to plastic pollution of rivers in recent years, could be agricultural plastic. Agricultural plastic wrap was, in Norway, introduced during the 1980's, to preserve hay and silo in plastic wrapped bales (Bollestad, 2020; Norsk landbruksrådgiving, N.D). Research done by Velle et al., 2020, show that 70% of the plastic found in 43 rivers along the west coast of Norway, comes from agricultural plastic. Agricultural plastic comes in many types and forms, the most common types according to Ranneklev et al., 2019:

- Plastic wrap made out of polyethylene (PE).
- Plastic straw bags made out of polypropylene (PP).
- Plastic nets made out of high density polyethylene (HDPE).

During the last decades measures have been taken to reduce the pollution of agricultural plastic into the rivers. Agricultural municipalities have offered to collect plastic waste, to reduce the risk of plastic getting lost and polluting the nature (Grønnpunkt-Norge, N.D).

The contribution of agricultural plastic in Drammensfjorden can not be determined at this point, due to lack of identified particles.

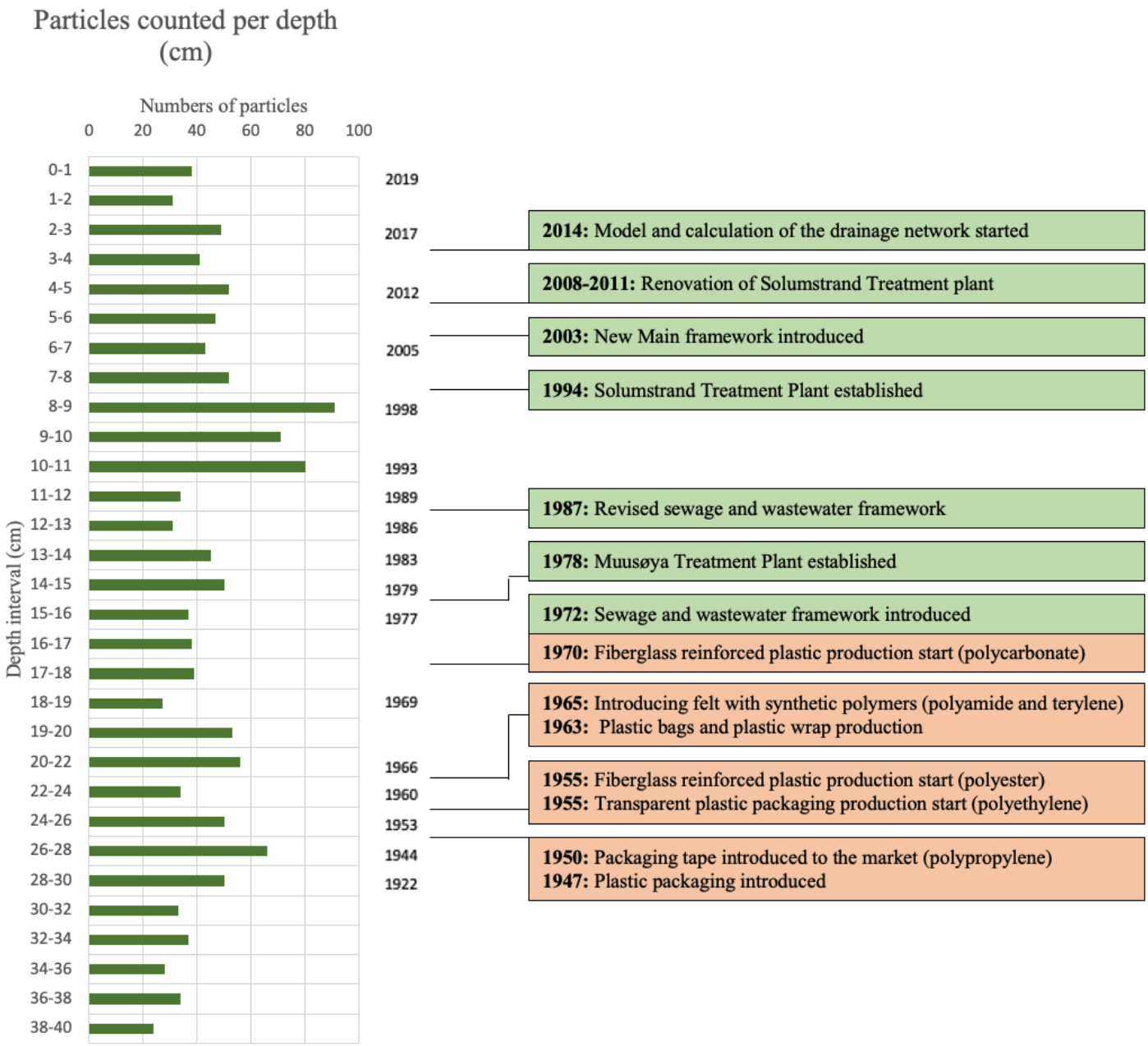

Figure 4.1: Microplastic counted in core DRA2A per sediment depth, with radiometric dating based on Ekeroth et al., 2020 and important events in the history of plastic evolution in Drammen (1.2.3).

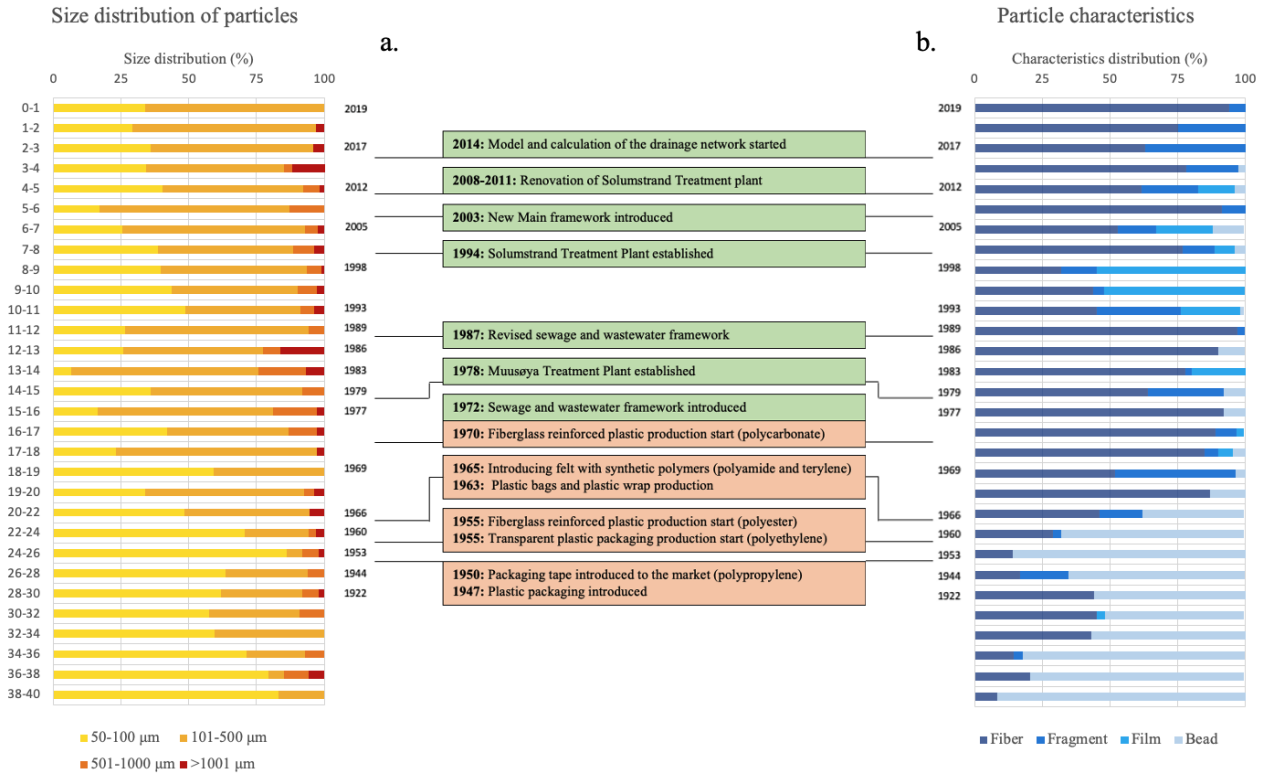

Figure 4.2: Size **a.** and shape **b.** distribution in core DRA2A per sediment depth, with important events in history of plastic production in Drammen.

4.3 Comparing microplastic accumulation in sediments at different water depths in Drammensfjoren.

Sediment cores were collected at two different locations in Drammesfjorden, August 25th 2020. DRA1 was collected at 60 meters water depth closer to the harbour in Drammen, while DRA2 was collected at 80 meters water depth further out in the fjord (Figure 4.3). Sediment cores collected at DRA1 were described and analysed in Thorstensen, 2021.

The difference in microplastic observed at the two locations is significant, where there in core DRA1A (Thorstensen, 2021) were observed over 250 particles at several depths. Sediment core DRA2A did not exceed 100 particles per depth interval. Most types of plastics have higher densities than seawater (1.03 gcm^{-3}), and will sink relatively fast, if not transported by streams. By looking at the microplastic characteristics, the distribution between different shapes are not as prominent in DRA1A as it varies a lot, except for the bottom 10 cm, where beads dominates. For DRA2A, fibers dominate the top 20 cm of the core, and beads the bottom 20 cm. It should be noted that the dating of the two cores are different, as the sedimentation in core DRA1A have occurred in a shorter period of time. The domination of microplastic beads in both cores are dated to the 1960's, even though there is a 10 cm difference in sediment depths.

Figure 4.3: Sediment core sampling locations in Drammensfjorden, August 2020.

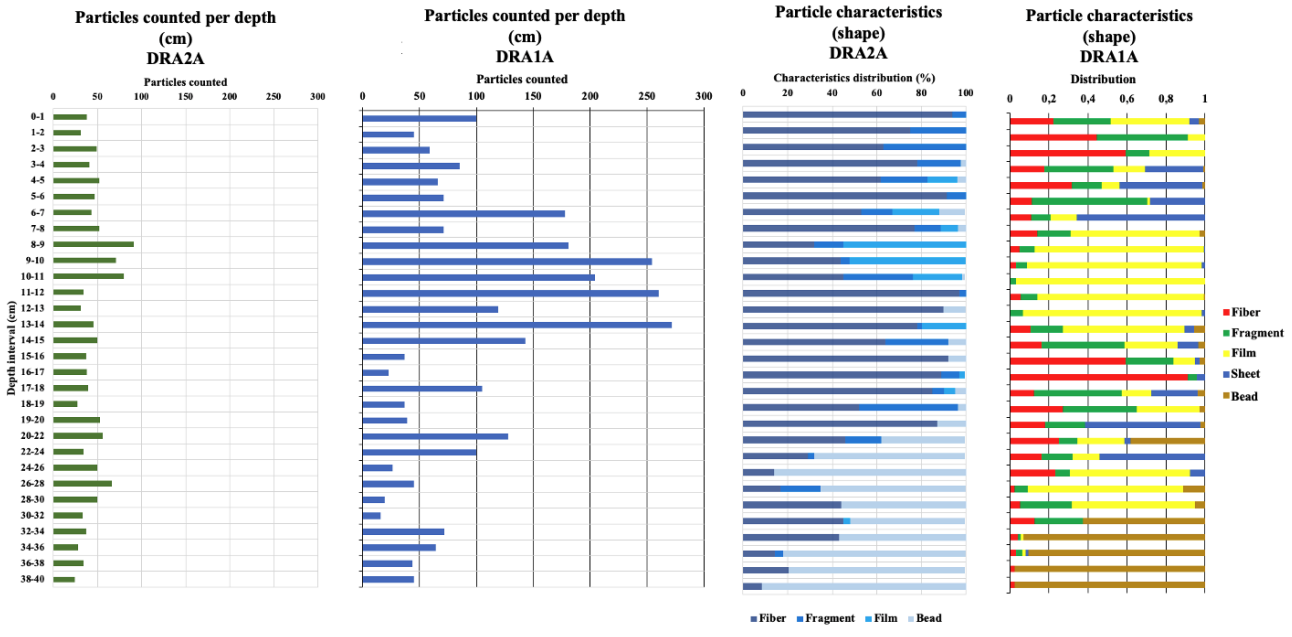

Figure 4.4: Microplastic count in **a.** DRA2A and DRA1A **b.** per sediment depth. Particle characteristics distribution for **c.** DRA2A and **d.** DRA1A. Data for core DRA1A modified after Thorstensen, 2021.

The difference in sedimentation rate can be explained by the distance from shore and depth of the two sampling locations. The particles could be transported in several ways, by suspended load transport, saltation or traction transport. The lighter particles gets transported further from shore by suspension, where currents disturb material close to the seabed, and force the particles upward and keeps them suspended in the water column for longer periods (Boggs Jr, 2014). With the mechanism of suspension this allows lighter particles to be transported further, and might be the case for the accumulated material in DRA2A, where the majority of particles were smaller fibers.

4.4 Improvement in the environmental condition of the fjord during the last decade?

The environmental condition, or the ecological condition, of the fjord is, according to The Norwegian Water Resources and Energy Directorate (NVE), 2021b, described as "bad". By looking at the oxygen content measured in August 2020, the amount of oxygen reaching the seafloor at greater depths are limited (Figure 3.1). The low oxygen content near the seafloor indicates low circulation in the deeper layers of seawater and can therefore cause anoxic conditions in the sediment . The low rate of bioturbation in the upper layers of the sampled sediment cores, can corroborate this assumption, as most organisms tend to live in well oxygenated environments (Arnesen, 2001). Research done by Smittenberg et al., 2005 indicated anoxic or poorly oxygenated condition in the deeper areas of the fjord during the last 1000 years. Oxygen and salinity measurements by Norconsult for Fylkesmannen i Buskerud in 2014-2015, also indicated little to no change in both oxygen concentration, and salinity from November 2014 to June 2015, for layers deeper than 30 m (Fylkesmannen_Buskerud, 2016).

Table 4.3: Classification of oxygen in deep seawater, modified from Fylkesmannen_Buskerud, 2016.

Parameter	I Very good	II Good	III Moderate	IV Bad	V Very bad
Oxygen (mL O_2/L)	>4.5	4.5-3.5	3.5-2.5	2.5-1.5	<1.5
Oxygen (%)*	> 65	65-50	50-35	35-20	<20

* Calculated with salinity 33 and temperature 6 °C.

Comparing the measured oxygen during sampling, with the classification in Table 4.3 indicates that the condition in the deeper layers of seawater are "Very bad". The measured oxygen at DRA2 at 78.92 meters depth was 11.72 %, which is $< 20\%$ and equals to "Very bad". From 58.73 meters depth the amount of oxygen is $< 20\%$.

The concentration of oxygen in the deeper layers of the fjord can not give an indication of the environmental condition of the fjord, due to lack of circulation in the deeper layers of the water column. The fjord in itself is almost cut off from the larger Oslo fjord by the glacial moraine at Svelvik, which cause low circulation in deep seawater. (Hvoslef et al., 1987).

5 Conclusion and Further work

- The amount of counted microplastic in the sediment core increase downwards, indicating less contamination of plastic in recent years.
- The industrialisation of Drammen appears to have had an impact on the accumulation of microplastic in the sediments, the impact can't be seen in the amount of accumulated plastic, but rather in the type and size of the particles. Microplastics accumulated before the industrialisation, were mainly smaller beads in the size range 50-100 µm. After the industrialisation the majority of accumulated microplastic were small fibers in the size range 50-500 µm.
- The lack of identification of microplastic by using Raman and ATR-FTIR spectroscopy, makes it impossible to determine the direct source of microplastic contamination into the fjord. The change in type of microplastic after industrialisation can confirm that the industry have been a significant factor in the microplastic contamination of the fjord.
- Sewage and wastewater framework introduced by the municipality of Drammen, and the establishment of treatment plants in the Drammen area have a direct correlation with the amount of accumulated microplastic in the sediments.
- The accumulation of microplastic in the sedimnents show larger amounts of plastic deposited near shore (DRA1), than further out in the fjord (DRA2). The difference in microplastic types for the two locations can be explained by suspension, where lighter particles, in this case fibers, are transported further out in the fjord (DRA2), than fragments which are more present closer to shore (DRA1).
- Th environmental condition of the fjord by looking at the oxygen content in deep seawater layers, can't reveal the actual environmental condition, due to the low circulation deeper parts of the fjord caused by the glacial moraines at Svelvik.

Further work should include new collections of samples in Drammensfjorden, as there were procedual challenges, including the formation of tri-iodide which impacts the effectiveness of the sample processing. The approach used to extract the microplastic from the samples should be reconsidered or carried out more thoroughly, to ensure oxidation of iodide and hydrogen peroxide to not occur.

For this exact location it would be beneficial to have radiometric dating for the whole core, for better understanding of the accumulation of plastic in the sediment, before polymers were introduced to the industry.

6 References

References

Andrady, A. L. (2011). "Microplastics in the Marine Environment". In: *Marine Pollution Bulletin* vol. 63, pp. 1596–1605.

Arnesen, V. (2001). "The pollution and protection of the inner Oslofjord: redefining the goals of wastewater treatment policy in the 20th century". In: *AMBIO: A Journal of the Human Environment* vol. 30, no. 4, pp. 282–286.

Arthur, C., Baker, J. E., and Bamford, H. A. (2009). "Proceedings of the International Research Workshop on the Occurrence, Effects, and Fate of Microplastic Marine Debris, September 9-11, 2008, University of Washington Tacoma, Tacoma, WA, USA". In:

Boggs Jr, S. (2014). *Principles of sedimentology and stratigraphy*. Pearson Education.

Bollestad, O. V. (2020). *Svar på skriftlig spørsmål om forsøpling fra rundballeplast*. URL: https://www.regjeringen.no/no/aktuelt/svar-pa-skriftlig-sporsmal-om-forsopling-fra-rundballeplast/id2788773/ (visited on 08/25/2021).

Borgen, P. O. (2004a). *Christensen, P., Tricotagefabrikk, Drammen byleksikon*. URL: http://byleksikon.drmk.no/christensen-p-tricotagefabrik/ (visited on 08/08/2021).

— (2004b). *Drammens cichorifabrikker. Drammen byleksikon*. URL: https://byleksikon.drmk.no/drammens-cichorifabrikker/ (visited on 10/29/2020).

— (2004c). *Star Paper Mill A/S (Stargruppen), Drammen byleksikon*. URL: http://byleksikon.drmk.no/star-paper-mill-as/ (visited on 08/08/2021).

— (2004d). *Tico A/S, Drammen byleksikon*. URL: http://byleksikon.drmk.no/ticon-as/ (visited on 08/08/2021).

Borgen, P. O. (2011). *Made in Drammen: Industrihistorie fra en østlandsby med hovedvekt på perioden 1870-1970*. Drammen Rotary.

Borrelle, S. B., Ringma, J., Law, K. L., Monnahan, C. C., Lebreton, L., McGivern, A., Murphy, E., Jambeck, J., Leonard, G. H., Hilleary, M. A., et al. (2020). "Predicted growth in plastic waste exceeds efforts to mitigate plastic pollution". In: *Science* vol. 369, no. 6510, pp. 1515–1518.

Bürgi, T. (2011). "Attenuated total reflection infrared (ATR-IR) spectroscopy, modulation excitation spectroscopy (MES), and vibrational circular dichroism (VCD)". In: *Biointerface Characterization by Advanced IR Spectroscopy*. Elsevier, pp. 115–144.

Cole, M., Lindeque, P., Halsband, C., and Galloway, T. S. (2011). "Microplastics as contaminants in the marine environment: a review". In: *Marine pollution bulletin* vol. 62, no. 12, pp. 2588–2597.

Crespy, D., Bozonnet, M., and Meier, M. (2008). "100 Years of Bakelite, the Material of a 1000 Uses". In: *Angewandte Chemie International Edition* vol. 47, no. 18, pp. 3322–3328.

Davis, H. (2015). "Life and death in the Anthropocene: A short history of plastic". In: *Art in the anthropocene: Encounters among aesthetics, politics, environments and epistemologies*, pp. 347–58.

Disha, N., Bhawana, P., Fulekar, M., et al. (2012). "Production of Biodegradable Plastic from Waste Using Microbial Technology". In: *International Journal of Research in Chemistry and Environment* vol. 2, no. 2, pp. 118–123.

DrammenKommune (2018). *Kommunedelplan for kulturminner og kulturmiljøer.* URL: https://www.drammen.kommune.no/globalassets/tjenester/arealplan-kart-og-geodata/dokumenter/gjeldende-kommuneplaner/kommunedelplaner-drammen/kulturminneplan-2018.pdf (visited on 08/14/2021).

Ekeroth, N., Hjort, T., and Stubø, E. (Apr. 2020). "Ren Drammensfjord, sedimentundersøkelse 2019". In: *Drammen og Lier kommune*, p. 233.

Enders, K., Lenz, R., Stedmon, C. A., and Nielsen, T. G. (2015). "Abundance, size and polymer composition of marine microplastics 10 μm in the Atlantic Ocean and their modelled vertical distribution". In: *Marine pollution bulletin* vol. 100, no. 1, pp. 70–81.

Fredriksen, H. (1966). *Revolusjonerende utvikling... Mer enn 50 år med gummi.* NGF - Norges Gummitekniske Forening.

Frias, J., Pagter, E., Nash, R., O'Connor, I., Carretero, O., Filgueiras, A., Viñas, L., Gago, J., Antunes, J., Bessa, F., et al. (2018). "Standardised protocol for monitoring microplastics in sediments. Deliverable 4.2." In:

Fylkesmannen_Buskerud (2016). *Miljøovervåking av Indre Drammensfjord, Årsrapport 2015.* URL: https://www.statsforvalteren.no/siteassets/utgatt/fm-buskerud/dokument-fmbu/miljo-og-klima/sedimentopprydding---ren-drammensfjord/arsrapporter/rapport_miljoovervaking_drammensfjord_2015_j04.pdf (visited on 08/27/2021).

Geyer, R., Jambeck, J. R., and Law, K. L. (2017). "Production, use, and fate of all plastics ever made". In: *Science advances* vol. 3, no. 7, e1700782.

Gregory, M. R. and Andrady, A. L. (2003). *Plastics and the environment.* John Wiley and sons.

Grønnpunkt-Norge (N.D). *Landbruk.* URL: https://www.grontpunkt.no/gjenvinning/plastemballasje-naeringsliv-landbruk/landbruk/ (visited on 08/25/2021).

Heieren, R. (2004a). *Drammen paper mills A/S, Drammen byleksikon.* URL: http://byleksikon.drmk.no/drammen-paper-mills-as/ (visited on 10/29/2020).

— (2004b). *Refsums Gummivarefabrikk, Drammen byleksikon.* URL: https://byleksikon.drmk.no/refsums-gummivarefabrik/ (visited on 08/08/2021).

— (2004c). *Vokspapirfabrikken (VOPA) A/S, Drammen byleksikon.* URL: http://byleksikon.drmk.no/vokspapirfabrikk-en-vopa-as/ (visited on 08/08/2021).

— (2020a). *Birger Næss Plastvarefabrikk, Drammen byleksikon.* URL: https://byleksikon.drmk.no/birger-naess-plastvarefabrikk/ (visited on 08/08/2021).

— (2020b). *Jul-i-Nor, Nils Gulhaug A/S, Drammen byleksikon.* URL: https://byleksikon.drmk.no/jul-i-nor-nils-gulhaugen-a-s/ (visited on 08/08/2021).

— (2020c). *Transparent Emballasje A/S, Drammen byleksikon.* URL: https://byleksikon.drmk.no/transparent-emballasje-a-s/ (visited on 08/08/2021).

Hurley, R. R., Lusher, A. L., Olsen, M., and Nizzetto, L. (2018). "Validation of a method for extracting microplastics from complex, organic-rich, environ-

mental matrices". In: *Environmental science & technology* vol. 52, no. 13, pp. 7409–7417.

Hurley, R., Woodward, J., and Rothwell, J. J. (2018). "Microplastic contamination of river beds significantly reduced by catchment-wide flooding". In: *Nature Geoscience* vol. 11, no. 4, pp. 251–257.

Hvoslef, S., Kirkerud, L., Knutzen, J., Kvalvågnæs, K., Magnusson, J., Mjelde, M., Næs, K., Pedersen, A., Rygg, B., and Wiik, Ø. (1987). "Basisundersøkelser i Drammensfjorden 1982-84 Konklusjonsrapport". In:

Industrimuseum.no (N.D). *Drammen. Teknisk museum Oslo.* URL: `http://industrimuseum.no/omrader/drammen` (visited on 10/28/2020).

Jambeck, J. R., Geyer, R., Wilcox, C., Siegler, T. R., Perryman, M., Andrady, A., Narayan, R., and Law, K. L. (2015). "Plastic waste inputs from land into the ocean". In: *Science* vol. 347, no. 6223, pp. 768–771.

Johnson, A. E. and Myers, A. B. (1996). "Solvent effects in the Raman spectra of the triiodide ion: observation of dynamic symmetry breaking and solvent degrees of freedom". In: *The Journal of Physical Chemistry* vol. 100, no. 19, pp. 7778–7788.

Kershaw, P., Turra, A., Galgani, F., et al. (2019). "Guidelines for the Monitoring and Assessment of Plastic Litter in the Ocean-GESAMP Reports and Studies No. 99". In: *GESAMP Reports and Studies*.

Kristoffersen K., D. n. p. (1966). *50 år i treforedlingsindustriens tjeneste: A/S Den norske papirfiltfabrik 1916-1966*. Fabrikken.

Lavoy, M. and Crossman, J. (2021). "A novel method for organic matter removal from samples containing microplastics". In: *Environmental Pollution* vol. 286, p. 117357.

Lusher, A. e. a. (2020). "Plastic analysis using visual identification". unpublished.

Mikutta, R., Kleber, M., Kaiser, K., and Jahn, R. (2005). "Organic matter removal from soils using hydrogen peroxide, sodium hypochlorite, and disodium peroxodisulfate". In: *Soil science society of America journal* vol. 69, no. 1, pp. 120–135.

NIVA (N.D). "2B-Extracting Microplastics from organic, Solid samples". unpublished.

Norsk landbruksrådgiving, L. N. (N.D). "Lagring av rundballar - Gode løysingar for gardbrukar og miljø". In: p. 20.

Ranneklev, S. B., Hurley, R., Bråte, I. L. N., and Vogelsang, C. (2019). "Plast i landbruket: kilder, massebalanse og spredning til lokale vannforekomster (Plastland)". In: *NIVA-rapport*.

Ribic, C. A., Sheavly, S. B., Rugg, D. J., and Erdmann, E. S. (2010). "Trends and drivers of marine debris on the Atlantic coast of the United States 1997–2007". In: *Marine pollution bulletin* vol. 60, no. 8, pp. 1231–1242.

Shah, A. A., Hasan, F., Hameed, A., and Ahmed, S. (2008). "Biological degradation of plastics: a comprehensive review". In: *Biotechnology advances* vol. 26, no. 3, pp. 246–265.

Siesler, H. K. and Holland-Moritz, K. (1980). *Practical Spectroscopy series Volume 4; Infrared and Raman Spectroscopy of Polymers*. Marcel Dekker, inc.

Smittenberg, R. H., Baas, M., Green, M. J., Hopmans, E. C., Schouten, S., and Damsté, J. S. (2005). "Pre-and post-industrial environmental changes as revealed by the biogeochemical sedimentary record of Drammensfjord, Norway". In: *Marine Geology* vol. 214, no. 1-3, pp. 177–200.

Spigseth, K. and Miljøverndepartementet (2007). *Byutviklingsprossesene i Drammen*. URL: https://www.baerum.kommune.no/globalassets/aktuelt/dokumenter/md---byutvikling-drammen_v3.pdf (visited on 07/28/2021).

The Norwegian Water Resources and Energy Directorate (NVE) (Aug. 5, 2021a). *NEVINA*.

— (Aug. 27, 2021b). *Vann-nett, Indre Drammensfjord*.

Thompson, R. C., Olsen, Y., Mitchell, R. P., Davis, A., Rowland, S. J., John, A. W., McGonigle, D., Russell, A. E., et al. (2004). "Lost at sea: where is all the plastic?" In: *Science(Washington)* vol. 304, no. 5672, p. 838.

Thorstensen, M. (2021). "Tilstand indre Drammensfjord og historisk akkumulasjon av mikroplast i fjordsedimenter." Sem Sælandsvei 1, 0371 Oslo.

TracesCentre (2021). "Understanding Raman Spectroscopy, Principles and Theory, Version 5". In: *University of Toronto at Scarborough*, pp. 1–5.

Velle, G., Barlaup, B., Espedal, E. O., Haave, M., Landro, Y., Normann, E., Postler, C., Skoglund, H., Stranzl, S., Stöger, E., et al. (2020). "Plast i elver på Vestlandet". In:

Watson, R., Revenga, C., and Kura, Y. (2006). "Fishing gear associated with global marine catches, I. Database development". In: *Science Direct, Fisheries Reserach* vol. 79, pp. 97–102.

Wøhni, A. (2007). *Temarapport: Byutviklingen i Drammen, Langsiktig arbeid for miljøvennlig bysentrum.* Miljøverndepartementet, Oslo.

Ziccardi, L. M., Edgington, A., Hentz, H., Kulacki, K. J., and Driscoll, S. K. (2016). "Microplastics as vectors for bioaccumulation of Hydrophobic organic chemicals in the Marine Environment: A-state-of-the-Science Review". In: *Environmental Toxicology and Chemistry* vol. 35, no. 7, pp. 1667–1676.

Aagaard, K., Borgvang, S., and Strand, A. (2001). "Nedbørfeltdistrikter i Norge. Forslag til inndeling ut fra naturgeografiske og regionaladministrative forhold". In: *NINA oppdragsmelding* vol. 691, pp. 1–26.

7 Appendix

A Sediment core samples

Figure A.1: Marine sediment core logging scheme for sediment core 5BxA.

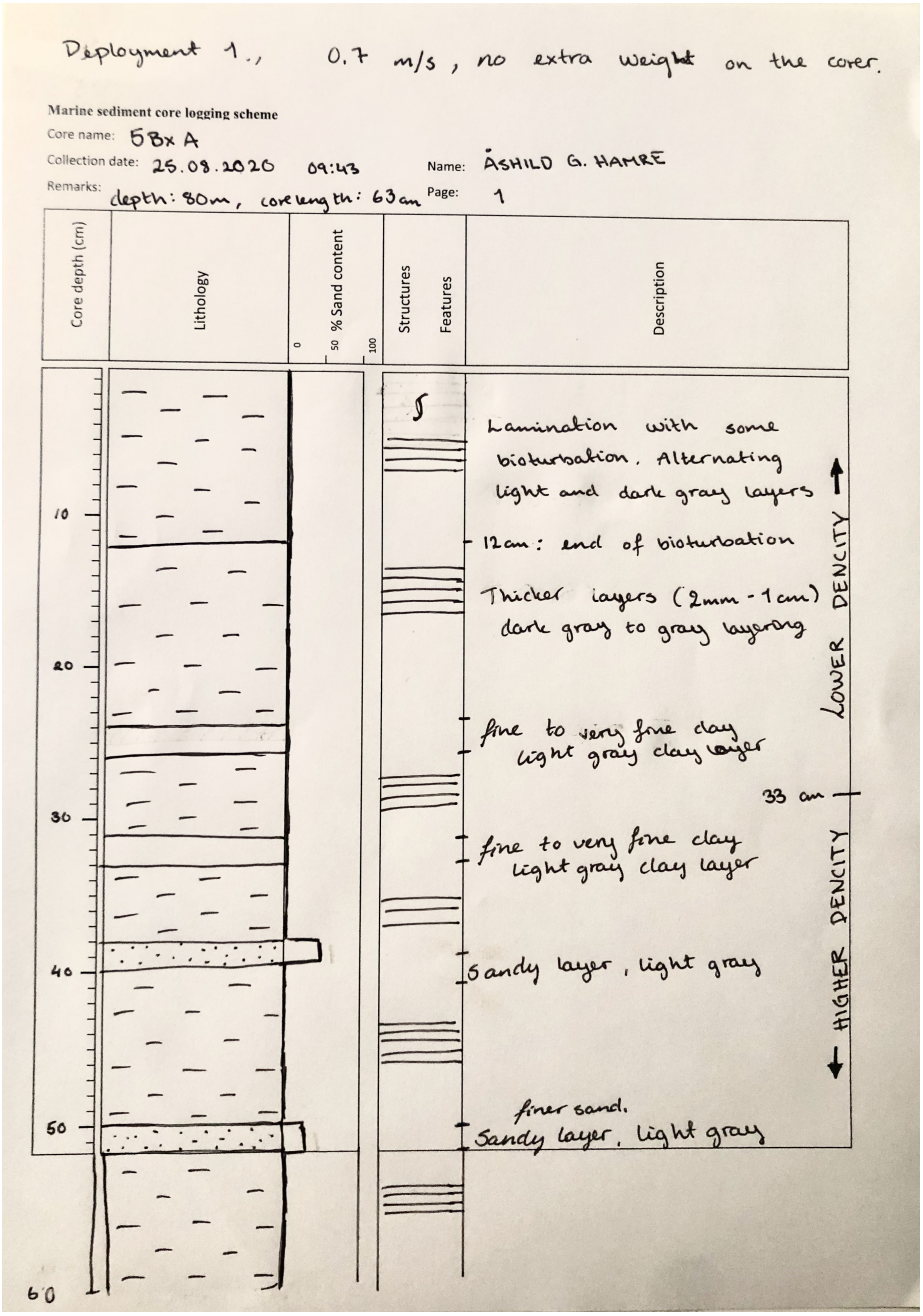

Table A.1: Sediment core description scheme, core 5BxF/DRA2B.

Station and core name: **5BxF/DRA2B**	Water depth (m): **80 m**	Latitude: **010°17.484'**	Longditude: **59°43.003'**
Sediment surface observations: **Bioturbation, brown surface**	Core length: **62 cm**	Sampling device: **Gemini twin corer**	

Date: 25.08.2020 **Weather conditions:** Sunny, slightly windy, 17°C

Core depth (cm)	Color	Treatment	Comments
0-1	Dark gray to black	Freezdryer	Brown sediment and bioturbation in the surface
1-2	Dark gray to black	Freezdryer	Black areas, some organic material
2-3	Dark gray with light gray areas	Freezdryer	Voids
3-4	Dark gray with black areas	Freezdryer	Shell, voids
4-5	Dark gray with black areas	Freezdryer	Many voids
5-6	Black with dark gray areas	Freezdryer	Voids, light gray areas
6-7	Black to dark gray	Freezdryer	Voids, light gray areas
7-8	Dark gray with black areas	Freezdryer	Voids
8-9	Homogeneous dark gray	Freezdryer	Light gray areas inside voids
9-10	Dark gray with black spots	Freezdryer	Voids
10-11	Homogeneous dark gray	Freezdryer	Sandy layer? Voids
11-12	Gray with black areas	Freezdryer	Voids
12-13	Homogeneous dark grey to black	Freezdryer	Voids
13-14	Gray to dark gray	Freezdryer	Voids
14-15	Homogeneous gray	Freezdryer	Voids
15-16	Dark gray	Freezdryer	Voids, fragments of rocks
16-17	Dark gray with black areas	Freezdryer	Less voids
17-18	Dark gray	Freezdryer	Less voids
18-19	Dark gray	Freezdryer	No voids
19-20	Homogeneous dark gray	Freezdryer	Oxidation around the edges
20-22	Dark gray with light gray areas	Freezdryer	Dense sediment
22-24	Gray	Freezdryer	Oxidation, fragment?

Core depth (cm)	Color	Treatment	Comments
24-26	Dark gray	Freezdryer	Fragment (Bryoso)
26-28	Gray	Freezdryer	Voids
28-30	Light gray	Freezdryer	Fine clay layer
30-32	Dark gray	Freezdryer	Fragment of rock
32-34	Dark gray to gray	Freezdryer	Homogeneous mass
34-36	Dark gray with some black areas	Freezdryer	Homogeneous
36-38	Dark gray	Freezdryer	Homogeneous
38-40	Homogeneous dark gray	Freezdryer	Organic fragment
40-44	Dark gray	Freezdryer	Homogeneous
44-48	Gray to dark gray	Freezdryer	Homogeneous
48-51	Gray to dark gray	Freezdryer	Homogeneous

Table A.2: Water content calculations for core DRA2A/5BxE.

Station name:	**DRA2/5Bx**	Core name:	**DRA2A/5BxE**
Water depth (m):	**80 m**	Sampling device:	**Gemini-twin-corer**
Latitude and	Longitude:	**010°17.484'**	**59°43.003'**

Core depth (cm)	interval	weight box (g)	weight box + wet sed. (g)	weight wet sed. (g)	weight box + dry sed. (g)	weight dry sed. (g)	water content (%)	salt correction dry weight (g)
0-1	0.5	7.982	55.596	47.614	15.333	7.351	84.561	5.982
1-2	1.5	8.048	58.311	50.263	18.205	10.157	79.792	8.793
2-3	2.5	7.962	57.753	49.791	19.174	11.212	77.482	9.900
3-4	3.5	7.984	59.386	51.402	23.976	15.992	68.888	14.788
4-5	4.5	8.000	63.399	55.399	29.137	21.137	61.846	19.972
5-6	5.5	7.967	67.480	59.513	31.526	23.559	60.414	22.337
6-7	6.5	8.010	64.079	56.069	27.439	19.429	65.348	18.183
7-8	7.5	7.989	62.496	54.507	27.757	19.768	63.733	18.587
8-9	8.5	8.009	64.809	56.800	29.014	21.005	63.019	19.788
9-10	9.5	7.994	60.555	52.561	26.267	18.273	65.235	17.107
10-11	10.5	7.981	63.111	55.130	24.782	16.801	69.525	15.498
11-12	11.5	8.023	61.354	53.331	26.985	18.962	64.445	17.793
12-13	12.5	7.980	60.613	52.633	26.999	19.019	63.865	17.876
13-14	13.5	7.985	68.342	60.357	29.893	21.908	63.703	20.601
14-15	14.5	7.994	59.474	51.480	26.282	18.288	64.476	17.159
15-16	15.5	7.993	67.849	59.856	28.048	20.055	66.495	18.702
16-17	16.5	8.010	68.265	60.255	29.690	21.680	64.020	20.368
17-18	17.5	7.985	67.946	59.961	28.655	20.670	65.528	19.334
18-19	18.5	8.007	74.601	66.594	42.059	34.052	48.866	32.946
19-20	19.5	8.011	64.969	56.958	24.290	16.279	71.419	14.896
20-22	21.0	8.001	128.972	120.971	49.630	41.629	65.588	38.931
22-24	23.0	8.099	139.931	131.832	64.086	55.987	57.532	53.408
24-26	25.0	8.132	137.472	129.340	61.599	53.467	58.662	50.887
26-28	27.0	8.112	138.746	130.634	66.228	58.116	55.512	55.650
28-30	29.0	8.112	142.703	134.591	72.018	63.906	52.518	61.503
30-32	31.0	8.118	137.243	129.125	67.812	59.694	53.770	57.333
32-34	33.0	8.110	137.850	129.740	65.705	57.595	55.607	55.142
34-36	35.0	8.115	129.097	120.982	60.224	52.109	56.928	49.767
36-38	37.0	8.108	137.491	129.383	68.886	60.778	53.025	58.445
38-40	39.0	8.110	148.169	140.059	82.713	74.603	46.735	72.377
40-44	42.0	3.494	289.271	285.777	162.952	159.458	44.20	155.163
44-48	46.0	3.561	263.001	259.440	142.308	138.747	46.52	134.643
48-50,5	49.25	3.583	195.505	191.922	104.673	101.090	47.33	98.002

Table A.3: Water content calculations for core DRA2B/5BxF.

Station name:	**DRA2/5Bx**	Core name:	**DRA2B/5BxF**
Water depth (m):	**80 m**	Sampling device:	**Gemini-twin-corer**
Latitude and	Longitude:	**010°17.484'**	**59°43.003'**

Core depth (cm)	interval	weight box (g)	weight box + wet sed. (g)	weight wet sed. (g)	weight box + dry sed. (g)	weight dry sed. (g)	water content (%)	salt correction dry weight (g)
0-1	0,5	8,117	69,085	60,968	18,491	10,374	82,985	8,654
1-2	1,5	8,099	67,300	59,201	20,246	12,147	79,482	10,547
2-3	2,5	8,160	68,859	60,699	23,238	15,078	75,159	13,527
3-4	3,5	8,094	69,499	61,405	29,746	21,652	64,739	20,300
4-5	4,5	8,107	73,071	64,964	32,265	24,158	62,813	22,771
5-6	5,5	8,132	75,983	67,851	28,982	20,850	69,271	19,252
6-7	6,5	8,111	76,706	68,595	33,431	25,320	63,088	23,849
7-8	7,5	8,118	68,562	60,444	27,154	19,036	68,506	17,628
8-9	8,5	8,127	67,921	59,794	26,817	18,690	68,743	17,292
9-10	9,5	8,097	73,117	65,020	29,286	21,189	67,412	19,699
10-11	10,5	8,119	71,869	63,750	31,465	23,346	63,379	21,972
11-12	11,5	8,093	71,134	63,041	31,116	23,023	63,479	21,662
12-13	12,5	8,100	68,613	60,513	29,605	21,505	64,462	20,179
13-14	13,5	8,126	74,054	65,928	30,386	22,260	66,236	20,775
14-15	14,5	8,085	70,919	62,834	30,885	22,800	63,714	21,439
15-16	15,5	8,120	69,524	61,404	29,857	21,737	64,600	20,388
16-17	16,5	8,110	71,463	63,353	38,676	30,566	51,753	29,451
17-18	17,5	7,996	63,882	55,886	24,235	16,239	70,943	14,891
18-19	18,5	8,013	66,089	58,076	26,041	18,028	68,958	16,666
19-20	19,5	7,982	74,863	66,881	33,602	25,620	61,693	24,217
20-22	21,0	8,005	139,555	131,550	62,260	54,255	58,757	51,627
22-24	23,0	7,993	144,584	136,591	64,130	56,137	58,901	53,402
24-26	25,0	7,980	136,908	128,928	59,138	51,158	60,320	48,514
26-28	27,0	8,012	152,487	144,475	77,201	69,189	52,110	66,629
28-30	29,0	7,987	145,805	137,818	75,586	67,599	50,951	65,212
30-32	31,0	7,989	141,628	133,639	76,151	68,162	48,995	65,936
32-34	33,0	8,027	135,466	127,439	64,416	56,389	55,752	53,973
34-36	35,0	7,984	146,719	138,735	77,922	69,938	49,589	67,599
36-38	37,0	8,004	154,107	146,103	94,903	86,899	40,522	84,886
38-40	39,0	7,964	149,349	141,385	85,854	77,890	44,909	75,731
40-44	42,0	3,433	287,513	284,080	175,055	171,622	39,59	167,798
44-48	46,0	3,519	286,755	283,236	171,539	168,020	40,68	164,103
48-51	49,5	3,534	233,551	230,017	123,905	120,371	47,67	116,643

B Plastic analysis - Visual

Table B.1: Visual observation, particle count for sediment core DRA2A at 0-1 cm water depth.

Site ID	Sample ID	Particle ID	Individual	Particle number	Color	Type	Length (µm)	Length (µm)	Date	Comment
DRA2A	DRA2A.0-1.1	A.0-1.1.1	1	1	black	fiber	100	10	03.02. 2021	
DRA2A		A.0-1.1.2	1	2	black	fiber	410	10	03.02. 2021	
DRA2A		A.0-1.1.3	2	3	black	fiber	65	10	03.02. 2021	
DRA2A		A.0-1.1.4	2	4	black	fiber	220	10	03.02. 2021	
DRA2A	DRA2A.0-1.2	A.0-1.2.1	1	5	black	fiber	140	10	03.02. 2021	
DRA2A		A.0-1.2.2	1	6	black	fiber	500	10	03.02. 2021	
DRA2A		A.0-1.2.3	2	7	blue/transp.	fiber	150	10	03.02. 2021	
DRA2A	DRA2A.0-1.3	A.0-1.3.1	1	8	black	fiber	210	10	03.02. 2021	
DRA2A		A.0-1.3.2	1	9	black	fiber	220	10	03.02. 2021	
DRA2A		A.0-1.3.3	2	10	gray/transp.	fiber	220	15	03.02. 2021	
DRA2A	DRA2A.0-1.4	A.0-1.4.1	1	11	black	fiber	60	10	03.02. 2021	
DRA2A		A.0-1.4.2	1	12	black	fiber	240	10	03.02.2021	
DRA2A		A.0-1.4.3	1	13	black	fiber	350	10	03.02.2021	
DRA2A		A.0-1.4.4	1	14	black	fiber	140	10	03.02.2021	
DRA2A		A.0-1.4.5	1	15	black	fiber	200	10	03.02.2021	
DRA2A		A.0-1.4.6	1	16	black	fiber	180	10	03.02.2021	
DRA2A		A.0-1.4.7	1	17	black	fiber	120	10	03.02.2021	
DRA2A		A.0-1.4.8	1	18	black	fiber	310	10	03.02.2021	
DRA2A		A.0-1.4.9	1	19	black	fiber	130	10	03.02.2021	
DRA2A		A.0-1.4.10	1	20	black	fiber	340	10	03.02.2021	
DRA2A		A.0-1.4.11	1	21	black	fiber	160	10	03.02.2021	
DRA2A		A.0-1.4.12	1	22	black	fiber	110	10	03.02.2021	
DRA2A		A.0-1.4.13	1	23	black	fiber	65	10	03.02.2021	
DRA2A		A.0-1.4.14	1	24	black	fiber	90	10	03.02.2021	
DRA2A		A.0-1.4.15	1	25	black	fiber	60	10	03.02.2021	
DRA2A		A.0-1.4.16	1	26	black	fiber	80	10	03.02.2021	
DRA2A		A.0-1.4.17	1	27	black	fiber	75	10	03.02.2021	
DRA2A		A.0-1.4.18	1	28	black	fiber	50	10	03.02.2021	
DRA2A		A.0-1.4.19	1	29	black	fiber	100	10	03.02.2021	
DRA2A		A.0-1.4.20	1	30	black	fiber	140	10	03.02.2021	
DRA2A		A.0-1.4.21	1	31	black	fiber	160	10	03.02.2021	
DRA2A		A.0-1.4.22	2	32	brown	fiber	80	10	03.02.2021	
DRA2A		A.0-1.4.23	2	33	brown	fiber	50	15	03.02.2021	
DRA2A		A.0-1.4.24	2	34	brown	fiber	90	15	03.02.2021	
DRA2A		A.0-1.4.25	2	35	brown	fiber	110	10	03.02.2021	
DRA2A		A.0-1.4.26	2	36	brown	fiber	120	10	03.02.2021	
DRA2A		A.0-1.4.27	3	37	black	fragment	240	240	03.02.2021	
DRA2A		A.0-1.4.28	2	38	black	fragment	180	160	03.02.2021	

Table B.2: Visual observation, summary; color distribution throughout the core DRA2A.

	Color (%)								
Depth (cm)	Black	Brown	White	Gray	Transparent	Red	Blue	Green	Yellow
0-1	85	13	2	0	0	0	0	0	0
1-2	78	13	0	0	3	3	0	3	0
2-3	69	6	0	2	2	2	0	15	4
3-4	71	0	5	2	12	0	5	5	0
4-5	21	23	12	6	0	0	2	35	2
5-6	81	2	11	0	0	0	0	6	0
6-7	40	12	30	2	0	5	2	9	0
7-8	56	2	10	19	0	0	0	13	0
8-9	27	1	49	8	1	1	0	12	0
9-10	39	0	54	3	0	0	0	1	3
10-11	50	14	24	3	0	3	0	6	1
11-12	91	0	0	0	0	6	0	3	0
12-13	81	0	3	3	0	3	0	0	10
13-14	69	4	20	0	0	0	0	4	2
14-15	88	0	4	2	0	0	0	6	0
15-16	86	0	3	3	0	3	0	3	3
16-17	82	0	0	5	0	5	3	5	0
17-18	84	3	8	0	0	0	0	5	0
18-19	74	22	0	0	0	0	0	4	0
19-20	89	4	0	6	0	0	0	0	2
20-22	89	0	4	2	2	0	2	2	0
22-24	71	15	9	0	0	0	0	6	0
24-26	84	0	10	0	6	0	0	0	0
26-28	59	2	17	2	0	0	2	12	8
28-30	81	6	0	5	2	0	0	2	4
30-32	67	24	3	3	0	0	0	3	0
32-34	43	3	54	0	0	0	0	0	0
34-36	21	7	64	4	0	0	4	0	0
36-38	73	0	15	6	0	3	0	3	0
38-40	63	8	8	21	0	0	0	0	0

Table B.3: Visual observation, summary; size and shape distribution throughout the core DRA2A.

	Size (%)				Shape (%)				
Depth (cm)	50-100µm	101-500µm	501-1000µm	>1001µm	Fiber	Fragment	Film	Bead	Particle count
0-1	34	66	0	0	94	6	0	0	38
1-2	29	68	0	3	75	25	0	0	31
2-3	36	60	0	4	63	37	0	0	49
3-4	34	51	3	12	78	20	0	2	41
4-5	40	52	6	2	62	21	13	4	52
5-6	17	70	13	0	91	9	0	0	47
6-7	26	67	5	2	53	14	21	12	43
7-8	38	50	8	4	77	12	8	4	52
8-9	40	54	5	1	32	13	55	0	91
9-10	44	46	7	3	44	4	52	0	71
10-11	49	43	5	4	45	31	22	1	80
11-12	26	68	6	0	97	3	0	0	34
12-13	26	52	6	16	90	0	0	10	31
13-14	7	69	18	7	78	2	20	0	45
14-15	36	56	8	0	64	28	0	8	50
15-16	16	65	16	3	92	0	0	8	37
16-17	42	45	11	3	89	8	3	0	38
17-18	23	74	0	3	85	5	5	5	39
18-19	59	41	0	0	52	44	0	4	27
19-20	34	58	4	4	87	0	0	13	53
20-22	48	46	0	5	46	16	0	38	56
22-24	71	24	3	3	29	3	0	68	34
24-26	86	6	6	2	14	0	0	86	50
26-28	64	30	6	0	17	18	0	65	66
28-30	62	30	6	2	44	0	0	56	50
30-32	58	33	9	0	45	0	3	52	33
32-24	59	41	0	0	43	0	0	57	37
34-36	71	21	7	0	14	4	0	82	28
36-38	79	6	9	6	21	0	0	79	34
38-40	83	17	0	0	8	0	0	92	24

Microplastic per gram dry sediment

Table B.4: Microplastic count per gram dry sediment, throughout core DRA2A.

Depth (cm)	Salt corrected dry weight (g)	Microplastic total	MP/g
0-1	5.982	38	6.352
1-2	8.793	31	3.523
2-3	9.900	49	4.949
3-4	14.788	41	2.603
4-5	19.972	52	2.603
5-6	22.337	47	2.104
6-7	18.183	43	2.364
7-8	18.587	52	2.797
8-9	19.788	91	4.598
9-10	17.107	71	4.150
10-11	15.498	80	5.162
11-12	17.793	34	1.910
12-13	17.876	31	1.734
13-14	20.601	45	2.184
14-15	17.159	50	2.913
15-16	18.702	37	1.978
16-17	20.368	38	1.865
17-18	19.334	39	2.017
18-19	32.946	27	0.819
19-20	14.896	53	3.558
20-22	38.931	56	1.438
22-24	53.408	34	0.636
24-26	50.887	50	0.982
26-28	55.650	66	1.185
28-30	61.503	50	0.812
30-32	57.333	33	0.575
32-34	55.142	37	0.670
34-36	49.767	28	0.562
36-38	58.445	34	0.581
38-40	72.377	24	0.331
Total	904.057	1361	
Average			1.505

Table B.5: Particles count obtained from Blank-tests. **Blank1** of filtered cleaning water, **5BXE** and **5BXF** from subsampling of cores Dra2A and Dra2B, and **DH1A** and **DH1H** from subsampling of cores DRA1A and DRA1B.

Sample	Sample ID	Particle ID	Shape	Size(µm)
Blank1	Blank1-1	Fiber	Red	1073
	Blank1-2	Fiber	Red	1653
	Blank1-3	Fiber	Grey	1295
	Blank1-4	Fiber	Blue	2165
5BXE	5BXE-1	Fiber	Blue	761
	5BXE-2	Fiber	Blue	946
	5BXE-3	Fiber	Blue	375
	5BXE-4	Fiber	Blue	1695
	5BXE-5	Fiber	Blue	919
	5BXE-6	Fiber	Blue	367
	5BXE-7	Fiber	Black	580
	5BXE-8	Fiber	Black	321
	5BXE-9	Fiber	Black	666
	5BXE-10	Fiber	Black	495
	5BXE-11	Fiber	Red	103
	5BXE-12	Fiber	Black	1011
	5BXE-13	Fiber	Black	1100
	5BXE-14	Fiber	Black	902
	5BXE-15	Fiber	Blue	2358
	5BXE-16	Fiber	Black	462
DH1A	DH1A-1	Fiber	Red	504
	DH1A-2	Fiber	Black	588
	DH1A-3	Fiber	Blue	470
	DH1A-4	Fiber	Black	294
	DH1A-5	Fiber	Blue	823
	DH1A-6	Fiber	Blue	1024
	DH1A-7	Fiber	Blue	965
	DH1A-8	Fiber	Red	1169
	DH1A-9	Fiber	Red	679
	DH1A-10	Fiber	Blue	1167
	DH1A-11	Fiber	Blue	1748
	DH1A-12	Fiber	Black	836
	DH1A-13	Fiber	Black	3579
	DH1A-14	Fiber	Grey	815
	DH1A-15	Fiber	Blue	832
	DH1A-16	Fiber	Black	647
	DH1A-17	Fiber	Black	375
	DH1A-18	Fiber	Blue	949
	DH1A-19	Fiber	Black	795
5BXF	5BXF-1	Fiber	Blue	4309
	5BXF-2	Fiber	Grey	892
	5BXF-3	Fiber	Clear	4037
DH1H	DH1H-1	Fiber	Blue	981
	DH1H-2	Fiber	Black	1409
	DH1H-3	Fiber	Blue	730
	DH1H-4	Fiber	Black	3152
	DH1H-5	Fiber	Blue	442
	DH1H-6	Fiber	Blue	1200
	DH1H-7	Fiber	Blue	993
	DH1H-8	Fiber	Red	369
	DH1H-9	Fiber	Blue	475
	DH1H-10	Fiber	Black	927

C Microplastic - Photographs

Figure C.1: Example of black fiber found in core DRA2A, here in sample A.2-3.1.**NOT IDENTIFIED or CARBON**.

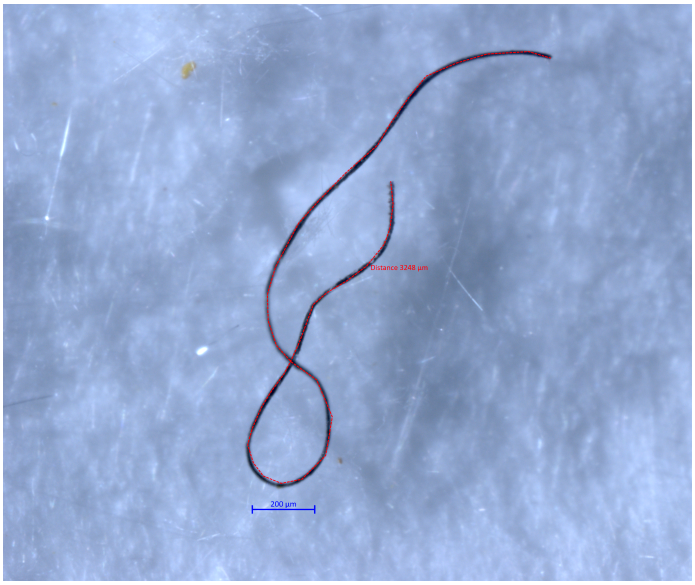

Figure C.2: Example of blue fiber found in core DRA2A, here in sample A.3-4.1.**ANTHROPOGENIC PIGMENT or POLYETHYLENE**.

Figure C.3: Example of white film found in core DRA2A, here in sample A.20-22.2. **NOT IDENTIFIED or SILICON RUBBER**.

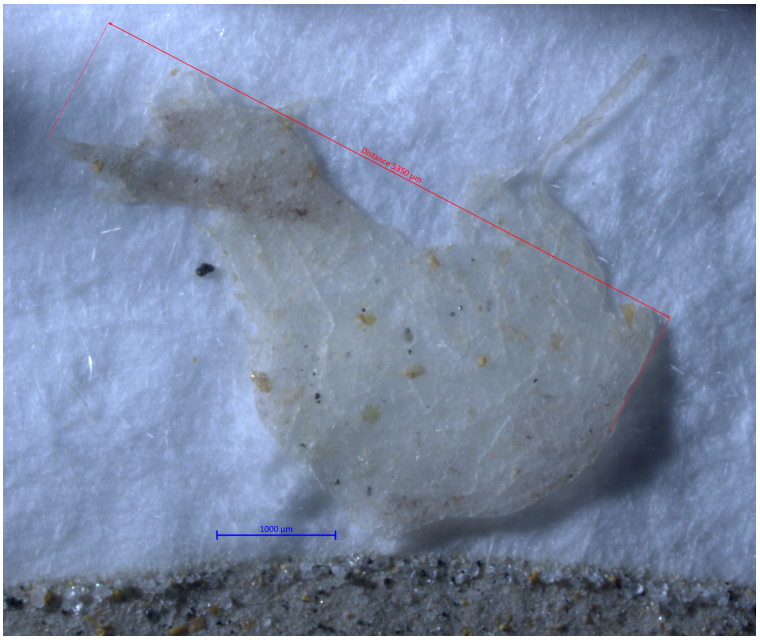

Figure C.4: Example of green fragment found in core DRA2A, here in sample A.26-28.3. **NOT IDENTIFIED**.

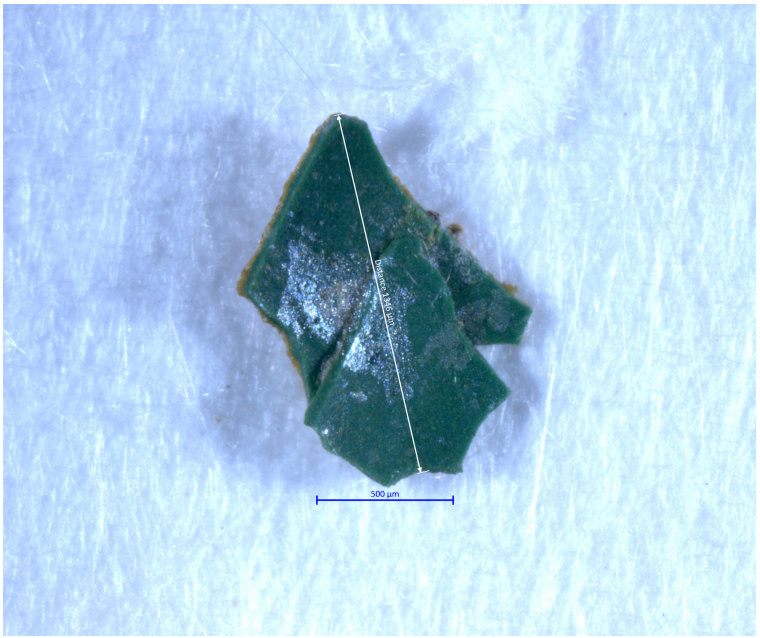

Figure C.5: Example of gray/brown fiber found in core DRA2A, here in sample A.30-32.2. **NOT IDENTIFIED**.

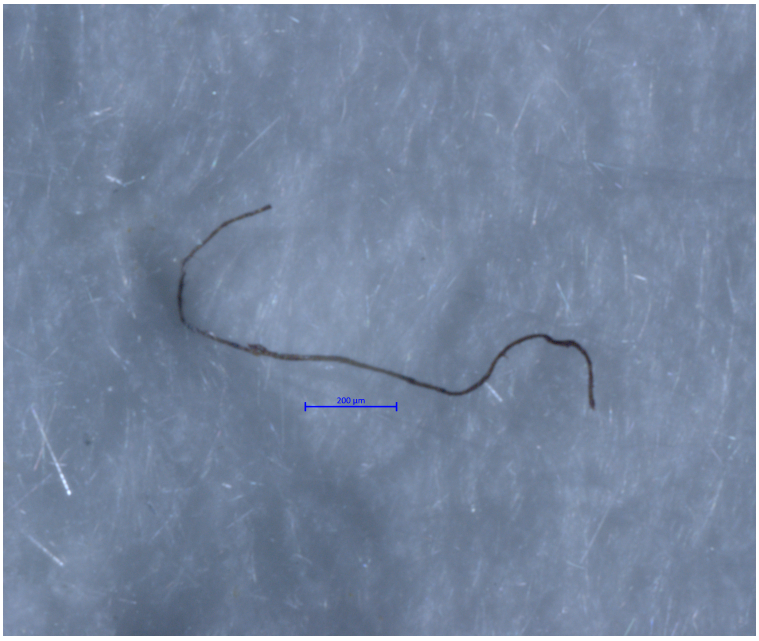

Figure C.6: Example of green fiber found in cor DRA2A, here in sample 16-17.3. **NOT IDENTIFIED**.

Figure C.7: Example of black bead found in core DRA2A, here in sample 38-40.3. **NOT IDENTIFIED**.